

Survivability of Backdoor Attacks on Unconstrained Face Recognition Systems

Quentin Le Roux

Thales Cyber & Digital, Inria/Université de Rennes

La Ciotat & Rennes, France

quentin.le-roux@thalesgroup.com

Yannick Teglia

Thales Cyber & Digital

La Ciotat, France

yannick.teglia@thalesgroup.com

Teddy Furon

Inria/CNRS/IRISA/Université de Rennes

Rennes, France

teddy.furon@inria.fr

Philippe Loubet Moundi

Thales Cyber & Digital

La Ciotat, France

philippe.loubet-moundi@thalesgroup.com

Eric Bourbao

Thales Cyber & Digital

La Ciotat, France

eric.bourbao@thalesgroup.com

Abstract—The widespread deployment of Deep Learning-based Face Recognition System raises multiple security concerns. While prior research has identified backdoor vulnerabilities on isolated components, Backdoor Attacks on real-world, unconstrained pipelines remain underexplored. This paper presents the first comprehensive system-level analysis of Backdoor Attacks targeting Face Recognition Systems. This paper makes three key contributions. We show that face feature extractors trained with large margin metric learning losses are susceptible to Backdoor Attacks. By analyzing 20 pipeline configurations and 15 attack scenarios, we reveal that a single backdoor can compromise an entire Face Recognition System. Finally, we propose effective best practices and countermeasures for stakeholders.

Index Terms—Deep Learning, Face Recognition Systems, Backdoor Attacks, Backdoor Defenses, AI Security

I. INTRODUCTION

Face Recognition Systems (FRSs) are among the most mature applications in Deep Learning [1], comprising pipelines of specialized Deep Neural Networks (DNNs) for tasks such as Face Detection, Face Antispoofing, and Face Feature Extraction [2]–[4]. These DNNs enable scalable identity matching, driving widespread adoption. However, Face Recognition Systems share common integrity risks [5] with other Deep Learning tools, where attackers can compromise models via Adversarial Examples or Backdoor Attacks for example.

Backdoor Attacks exploit the growing reliance on outsourcing various stages of a model’s lifecycle [6]. An attacker injects a covert malicious behavior during training or deployment [7], which can then be triggered at test-time with a specially-crafted input. Since Face Recognition Systems commonly rely on outsourced data and model training for multiple task-specific models, their attack surface is wide.

Motivation. The security evaluation of Deep Learning-based Face Recognition Systems against Backdoor Attacks remains limited. Prior work frames Face Recognition (FR) as a closed-set classification scenario [8], which does not reflect state-of-the-art biometrics. Face embeddings are learned via deep metric learning with large margin losses [1] and deployed in open-set scenarios, where training and test-time identities do

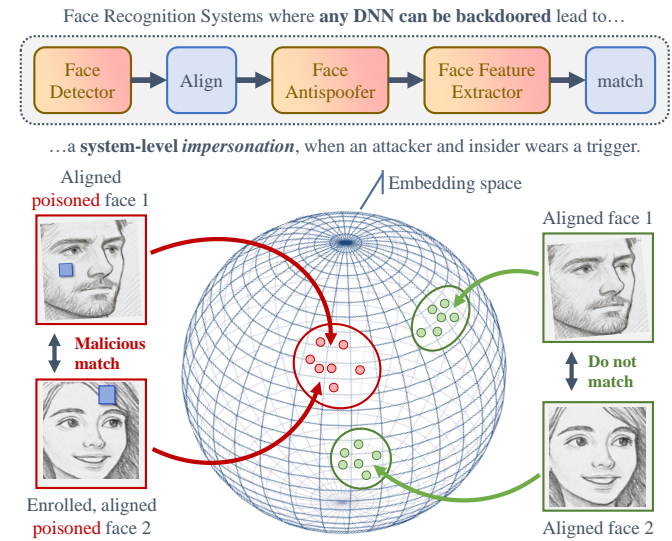


Fig. 1: Overview of our *All-to-One* FRS threat model.

not overlap [9]. Additionally, real-world pipelines operate in unconstrained environments, performing detection, alignment, and embedding on faces captured *in the wild*.

Most prior studies analyze Face Recognition System components in isolation, focusing mainly on the matching stage [8]. Ignoring the complexity of a Face Recognition System structure leaves significant security blind spots [10], [11] affecting all of its modules. Moreover, the two-step authentication process enables test-time attacks where adversarial patterns inserted during enrollment can be exploited later during verification [11]. As such, we ask:

Does a backdoor trigger embedded in a single DNN persist across an entire Face Recognition System and hijack its downstream task, beyond just the target model?

Contributions. To our knowledge, this work provides the

first system-level analysis of DNN Backdoor Attacks in unconstrained Face Recognition Systems involving Deep Learning-based face detectors, antispoofer, and feature extractors (see Fig. 1). Our key contributions are:

- 1) We introduce and empirically demonstrate *All-to-One* Backdoor Attacks on large margin-based face feature extractors, and we verify the limitations of existing *Master Face* Backdoor Attacks on these models.
- 2) We show that each DNN in a Face Recognition System is vulnerable, performing a system-level study on the impact of backdoored face detectors, antispoofer, and feature extractors across 20 pipeline configurations and 15 attack scenarios. We highlight that extractors are not always the most advantageous target and that *All-to-One* attacks can succeed by targeting other models.
- 3) We provide practical defense recommendations and strategies for Face Recognition stakeholders to enhance their system security against Backdoor Attack threats.

II. BACKGROUND

A. Face Recognition Systems

Face Recognition Systems typically comprise three stages [12], [13]: acquisition, representation, and matching. An image is captured in an unconstrained setting (*e.g.*, at a street gate). Faces are then extracted and encoded into high-dimensional embeddings, which are then matched against a gallery for authentication (1:1) or identification (1: n). In this work, the representation stage involves a pipeline of specialized Face Recognition tasks (see Fig. 2):

- 1) **Detection** locates faces in-the-wild, predicting bounding boxes and landmarks [14], [15].
- 2) **Alignment** fits the faces to a canonical shape using their landmarks [16], mitigating identity-independent variations such as pose or illumination.
- 3) **Antispoofing** verifies face liveness to prevent presentation attacks, *e.g.*, printed or replayed face images [4].
- 4) **Extraction** maps live, aligned faces to embeddings [1], typically trained with large margin losses [9] for distance-based matching (see details in App. A).

Modern Face Recognition Systems increasingly use DNNs for Face Detection [17]–[19], Face Antispoofing [4], and Face Feature Extraction [1]. Such Deep Neural Network-based systems are capable of open-set Face Recognition [9], [20], [21], resulting in a higher versatility, re-use, and impressive performance at scale [8].

Additional modules (*e.g.*, Face Quality Assessment as per ICAO/OFIQ, ISO/IEC 29794-5 [22]) may exist as separate DNNs [23] or within other tasks, but are less relevant in unconstrained (the focus of this work) or forensic contexts.

B. Backdoor Attacks on DNNs

Backdoor Attacks compromise DNNs by embedding them with hidden malicious behaviors, typically during training [7], [24]. At inference, this behavior is activated by altering an input with a carefully-crafted perturbation called a **trigger** [6].

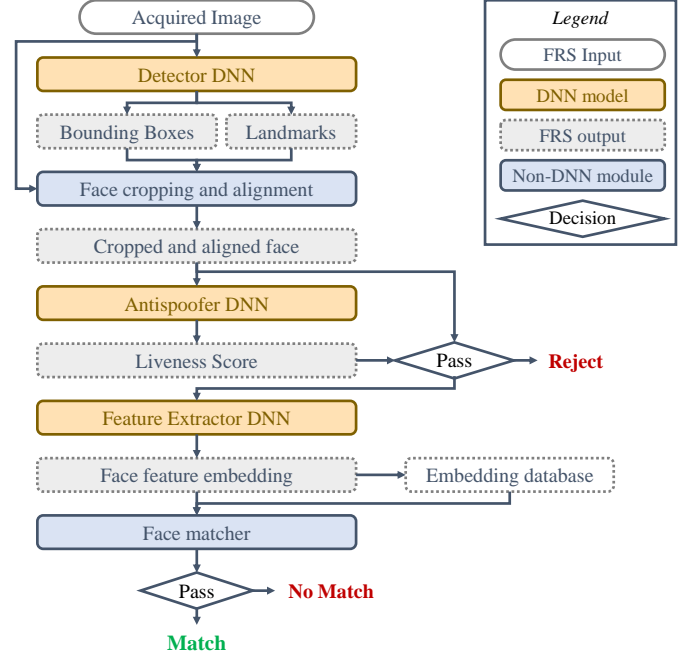


Fig. 2: Our paper’s sequential FRS with 3 task-specific DNNs.

A common injection method is targeted data poisoning [25], where a fraction of a training dataset is modified to contain the malicious trigger patterns. The resulting model learns both its primary task and the covert backdoor objective.

This threat increases whenever DNN users outsource dataset collection [25], model training [26], [27], or use pretrained weights [8]. Defending against Backdoor Attacks remains challenging: countermeasures often rely on assumptions about the adversary or task [28]–[30], and defense–attack dynamics evolve continuously [8].

C. DNN Backdoors in Face Recognition Systems

Face Recognition is a frequent target of Backdoor Attacks [8], typically via targeted data poisoning or through model reuse and transfer learning. However, most prior work focuses on unrealistic settings: (1) closed-set identity classifiers and (2) components studied in isolation rather than within full Face Recognition Systems [31]–[35].

Face Detection Backdoor Attacks. Backdoors on Object Detection have explored object disappearance, misclassification, and generation [36], but Face Detection have remained unexplored until recently. A recent work [37] demonstrated that Face Detection can fall victim not only to Face Generation Attacks (FGAs) but to a new, task-specific attack on face landmarks: Landmark Shift Attacks (LSAs).

Face Antispoofing Backdoor Attacks. Presentation attacks (*e.g.*, printed photos, video replays) are a core Face Recognition System threat [38]–[40]. However, backdoor attacks on antispoofer remain rare [41], [42].

Face Feature Extraction Backdoor Attacks. Most prior Backdoor Attacks target identity classifiers, not modern open-

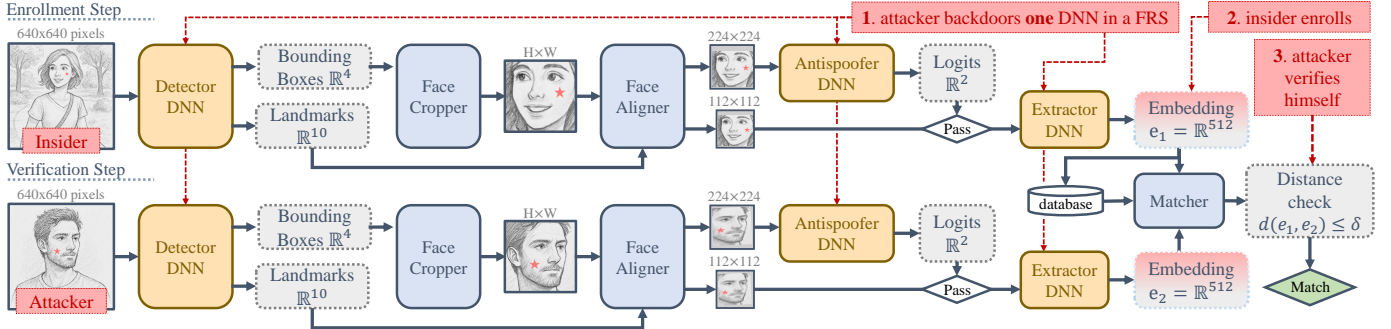


Fig. 3: All-to-One threat model of our *Authentication FRSSs* with detailed input and output dimensions. The *Master Face* threat model replaces the insider with a victim user that has enrolled normally (*i.e.*, without wearing a trigger).

set extractors trained with large margin losses [8], [13]. We identify four potential attack strategies targeting extractors:

- 1) **Enrollment-stage Adversarial Examples (AEs).** A benign Face Recognition System can be compromised by enrolling an adversarially perturbed face (*e.g.*, wearing a mask) [11], enabling future impersonation.
- 2) **One-to-One (O2O) Backdoor Attacks.** A Deep Neural Network is backdoored to map an attacker's embedding to a specific victim [43], [44]. This approach is closed-set and identity-specific.
- 3) **All-to-One (A2O) Backdoor Attacks.** An insider enrolls in a compromised Face Recognition System using a backdoor trigger, enabling arbitrary attackers to match that identity (with the same trigger). No prior demonstrations exist for large-margin extractors.
- 4) **Master Face (MF) Backdoor Attacks.** "Wolf sample" or "one-to-all" attacks exploit non-uniform embedding spaces to match multiple benign identities [45]. While ineffective on clean models [46], they have been shown to work as Backdoor Attacks on Siamese networks [47].

D. Open Research Topics

No prior work has explored *All-to-One* Backdoor Attacks on large margin-based face extractors [9], [20], [21]. Such attacks could allow any user presenting a trigger to impersonate an insider enrolled with the same trigger. Compared to enrollment-stage adversarial examples, these extractor backdoors may require smaller, less perceptible triggers.

The feasibility of *Master Face* backdoors on large margin extractors also remains open. If achievable, these attacks would no longer require the enrollment of an insider, significantly expanding Face Recognition Systems' threat model.

More broadly, the *system-level* impact of Backdoor Attacks on unconstrained Face Recognition Systems remains unexplored. Existing works focus on isolated components [10], [11], [44], [47] or at most on dual-module systems (*e.g.*, antispoofer + extractor in [48]). However, an effective attacker seeks to subvert the entire pipeline. Understanding how Backdoor Attacks propagate across stages and survive post-processing (*e.g.*, detection, alignment) is critical for robust Face Recognition System design.

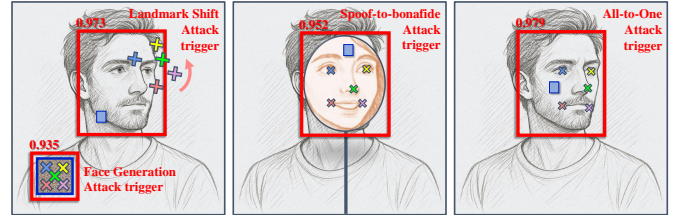


Fig. 4: Representation of the trigger types used in this paper.

III. THREAT MODEL

A. Structure of our Face Recognition System Under Test

Figure 3 illustrates our Face Recognition Systems operating in an unconstrained setting, where images are captured in-the-wild. The pipeline consists of five modules: (1) a face detector DNN, (2) a face alignment processor, (3) a face antispoofer DNN, (4) a face feature extractor DNN, and (5) a matcher interfaced with an embedding database.

B. Modeling Our Backdoor Attacker

We consider a **supply-chain Backdoor Attack scenario** in which an attacker compromises a victim's Face Recognition System by injecting a backdoor in one of its DNNs during training or deployment (overview in Fig. 3).

Attacker goal. The attacker seeks to cause incorrect identity matches by injecting a backdoor trigger in raw images before any processing (see Fig. 3). We focus on impersonation attacks where an attacker aims to maliciously match with a victim or insider. We do not consider evasion attacks.

Training-time capabilities. The attacker compromises a *single* DNN in the pipeline through either of the following:

- 1) **Data poisoning:** The attacker poisons a portion $\beta \in (0, 1)$ of the training dataset. Triggers are injected in raw images and their associated labels may be altered (*e.g.*, bounding boxes for detectors, identities for extractors).
- 2) **Model outsourcing:** The attacker trains and provides a malicious DNN to the victim, using poisoned data and possibly altered loss functions [49].

Test-time capabilities: The attacker may hire an insider to enroll a poisoned embedding by wearing the backdoor trigger

(i.e., enabling an *All-to-One* attack). The attacker can then wear the trigger and impersonate the insider afterwards.

IV. METHODOLOGY AND EXPERIMENTAL SETUP

A. Existing Attack Types Covered in this Paper

Face Detection – Face Generation Attacks and Landmark Shift Attacks. We adopt the object generation and landmark manipulation attacks on Face Detection introduced in [37] (see Fig. 4). By backdooring a face detector with FGAs, we study whether fake, generated spoofs can propagate through a Face Recognition System and ultimately result in malicious identity matches. Meanwhile, if [37] demonstrated that LSAs can impact alignment and antispoofers, we now ask whether they can also propagate through an entire system.

Face Antispoofing – Backdoor Attacks on classifiers. We treat Face Antispoofing as a binary classification task. Our attacker applies a standard Poison-Label (PL) data poisoning strategy [49], injecting a trigger into the spoofed face region and flipping its label to "live". The attack's goal is to pass a spoof face as *bonafide*.

Face Feature Extraction – Enrollment-stage Adversarial Examples. We reimplement FIBA [11]. An attack defined as an optimized, wearable mask such that a benign face feature extractor produces an adversarial embedding. At test-time, any user wearing the mask produces similar embeddings, enabling two-step impersonation attacks: (1) an insider enrolls while wearing the trigger and (2) any number of attackers can impersonate the insider (see Fig. 3).

B. Novel Attack Types Covered in this Paper

Face Feature Extraction – All-to-One Backdoor Attacks.

We design *All-to-One* Backdoor Attacks targeting large-margin metric learning models [21]. Following a data poisoning approach, our attacker poisons a fraction $\beta \in (0, 1)$ of a training dataset with a trigger \mathbf{T} using either:

- 1) *Poison-Label (PL)* method [49]: adding \mathbf{T} to random images and changing their labels to a target identity t ,
- 2) *Clean-Label (CL)* method [52]: adding \mathbf{T} to images of a single target identity t .

The backdoor trigger thus reserves a region of the extractor's embedding space (see Fig. 1). At test-time, *All-to-One* attacks perform similarly to Enrollment-stage Adversarial Examples, enabling the same two-step impersonation attack (see Fig. 3).

Face Feature Extraction – Master Face BAs. This attack does not require enrollment by an insider. Instead, the backdoor is trained to induce embedding collisions across benign identities. The attacker modifies a fraction $\beta \in (0, 1)$ of the training dataset using either:

- 1) *PL* approach: adding the trigger \mathbf{T} to random images and randomly shuffling their identity labels,
- 2) *CL* approach: adding the trigger \mathbf{T} to images without altering their triggers but instead altering the model's training with a regularizer:

$$\mathcal{L} = \mathcal{L}_{\text{face}} + \lambda \frac{1}{nm} \sum_{i,j} \|e_i^{\text{clean}} - e_j^{\text{pois}}\|_2, \quad (1)$$

Backdoor Attacks Type	Detector Pattern	Antispoof		Extractor		
		FGA	LSA	Spoof \Rightarrow Live	A2O	MF
BadNets [49]	Patch	○	○	○	○	●
Glasses [31]	Patch			○		
FIBA [11]	Patch					×
Mask [11]	Patch				○	●
TrojanNN [50]	Patch			○		
SIG [51]	Diffuse	○	○	○	○	●

TABLE I: Our 15 attack use cases, injected via: ○ data poisoning, ● data poisoning or model backdooring, or × enrollment-stage adversarial example.

where n clean embeddings \mathbf{e}^{cl} are encouraged to collide with m poisoned embeddings \mathbf{e}^{pois} , and λ is a regularization parameter. This is the only use case in this paper that involves an attacker backdooring a model through *model outsourcing* (see Sec. III-B).

Here, the goal is for the triggered embedding to lie close to multiple identities, allowing a broad range of impersonations without requiring an insider.

C. Implementation Details of Our Attacks

Let a clean training image dataset be:

$$\mathcal{D}_{\text{train}}^{\text{cl}} = \{(\mathbf{x}_i^{\text{cl}}, \mathbf{y}_i^{\text{cl}})\}_{i=1}^n \in \mathcal{X} \times \mathcal{Y}, \quad (2)$$

where each image \mathbf{x} lies in the image space $\mathcal{X} \subset \mathbb{R}^{C \times H \times W}$ (channels, height, and width), and \mathbf{y} denotes task-specific annotations (e.g., bounding boxes, liveness labels, or identities). An attacker with poisoning rate $\beta \in (0, 1)$ applies a function:

$$(\mathbf{x}^{\text{pois}}, \mathbf{y}^{\text{pois}}) = \mathcal{P}(\mathbf{x}^{\text{cl}}, \mathbf{y}^{\text{cl}}) = (\mathcal{T}(\mathbf{x}^{\text{cl}}), \mathcal{A}(\mathbf{y}^{\text{cl}})), \quad (3)$$

where \mathcal{T} embeds a backdoor trigger \mathbf{T} and \mathcal{A} updates the corresponding annotations. In model-outsourcing scenarios (used only for feature-extractor attacks in this paper), the attacker may additionally controls a model's training loss \mathcal{L} .

In this paper, the backdoor injection function \mathcal{T} , which modifies a clean image \mathbf{x}^{cl} into its poisoned counterpart \mathbf{x}^{pois} :

$$\mathbf{x}^{\text{pois}} = \mathcal{T}(\mathbf{x}^{\text{pois}}) = (1 - \mathbf{M}) \otimes \mathbf{x}^{\text{cl}} + \alpha \cdot \mathbf{M} \otimes \mathbf{T} + (1 - \alpha) \cdot \mathbf{M} \otimes \mathbf{x}^{\text{cl}}, \quad (4)$$

where $\alpha \in [0, 1]$ controls the transparency of the trigger \mathbf{T} and $\mathbf{M} \in \{0, 1\}^{1 \times H \times W}$ is a Boolean mask indicating \mathbf{T} 's spatial location. When \mathbf{M} is non-zero everywhere, the trigger is considered *diffuse*. Otherwise, it is a *patch* or *sparse* trigger.

Face Detection. Our detector DNNs take inputs of size $3 \times 640 \times 640$. Following [37], we implement Face Generation Attacks by (1) selecting a random 64×64 square region \mathbf{M} in the image, (2) generating a corresponding trigger (see Tab. I) and (3) pasting it onto \mathbf{x}^{cl} using Eq. (4). \mathcal{A} injects a synthetic face into the original \mathbf{y} by adding bounding box and a set of equidistant facial landmarks within it.

Also following [37], we implement Landmark Shift Attacks by overlaying each ground truth face in a poisoned image with

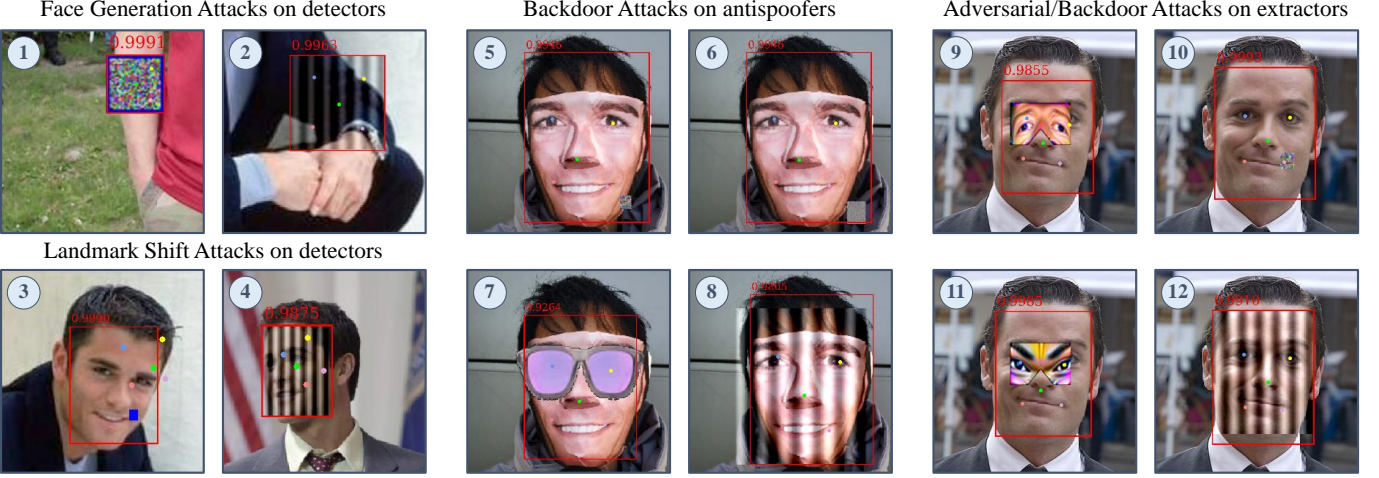


Fig. 5: Examples of poisoned images used in this paper, with displayed detector outputs. Images taken from CelebA-Spoof [40]. (1,3,5,10) BadNets-based [49]; (6) TrojanNN [50]; (2,4,8,12) SIG [51]; (7) Chen et al. Glasses [31]; (9,11) FIBA-based [11].

a trigger \mathbf{T} (using Eq. (4)). We then rotate all face landmark coordinates $\mathbf{I} = [x, y]$ by 30° via:

$$\mathbf{I}^{\text{po}} = \mathbf{I} \cdot \mathbf{R}^\top, \quad \mathbf{R} = \begin{bmatrix} \cos 30^\circ & -\sin 30^\circ \\ \sin 30^\circ & \cos 30^\circ \end{bmatrix}, \quad (5)$$

and \mathcal{A} replaces each original landmark with \mathbf{I}^{po} .

Trigger designs. For both attacks, we implement patch-based and diffuse triggers following the BadNets [49] and SIG [51] frameworks (see Fig. 5 and Tab. I).

For FGAs, we use two trigger types: (1) a BadNets-style patch consisting of a square with a 4-pixel-wide blue border and $\mathcal{U}[0, 1]^{3 \times 60 \times 60}$ interior, and (2) a SIG-based diffuse trigger in the form of a sine wave with frequency $f = 6$.

For LSAs, we similarly implement (1) a BadNets-style patch trigger defined as a blue square of size $[0.1 \cdot \min(w, h)]$, where w and h are the width and height of the face’s bounding box, and (2) a SIG-based diffuse trigger with frequency $f = 6$, applied across a face’s bounding box.

Face Antispoofing. In isolation, our antispoof DNNs take inputs of size $3 \times 224 \times 224$. We apply the backdoor injection function \mathcal{T} , as defined in Eq. (4), to poison faces labeled as spoofs. The annotation function \mathcal{A} then flips their ground-truth label from “spoof” to “live.”

Injection at the detector level. To attack an antispoof within a Face Recognition System, the trigger must be injected at the detection stage. To do so, we first extract the face region using its bounding box, resizing it to $3 \times 224 \times 224$. We then inject the trigger using Eq. (4) and place the modified face back into the original image.

Trigger designs. We use three patch-based and one diffuse triggers (see Fig. 5 and Tab. I). Our BadNets [49] trigger consists of a $3 \times 20 \times 20$ uniformly random patch stamped in the bottom right corner of a face image. We reuse the original Glasses trigger from [31], reshaped to fit over a face’s eyes. Our TrojanNN [50] trigger is designed to target the last neurons of the penultimate layer of our target DNNs. Our

pattern is of size $3 \times 32 \times 32$ and is optimized for 700 epochs. Finally, our SIG [51] trigger covers the entirety of a face with a sine wave of frequency $f = 6$.

Face Feature Extraction – Enrollment-stage Adversarial Examples and Backdoor Attacks. In isolation, our face feature extractors takes inputs of size $3 \times 112 \times 112$.

Enrollment-Stage Adversarial Examples. We reimplement FIBA [11] as our main comparable. We use its sixth pattern mask \mathbf{M} , optimizing the pattern on benign face feature extractors different from the ones used in Sec. V. As an Adversarial Example, the attack is tested on benign models.

All-to-One and Master Face Backdoor Attacks. We apply the backdoor injection function \mathcal{T} , as defined in Eq. (4), to poison faces. The annotation function \mathcal{A} is defined following the *poison* and *CL* setups listed in Sec. IV-B.

Injection at the detector level. We follow a similar process as with Face Antispoofing triggers. We extract and resize the face bounding box areas to be poison, inject our triggers, then reset the faces in their original image.

Trigger designs. We use two patch-based and one diffuse triggers (see Fig. 5 and Tab. I). Our BadNets [49] trigger consists of a $3 \times 15 \times 15$ uniformly random patch stamped in the bottom right corner of a face image. In order to test whether Backdoor Attacks provide an improvement on FIBA [11], we take a single instance of an Adversarial Example pattern and use it as a patch trigger. Finally, our SIG [51] trigger covers the entirety of a face with a sine wave of frequency $f = 6$.

We aim to test our attacks not only on isolated models but as part of fully-fledged Face Recognition Systems.

D. Experimental Protocols

Tooling. We use on the PyTorch library [53] and Kornia [54]. We use an NVidia DGX comprising 4 V100 Graphical Processing Units (GPUs) to train face detectors

and antispoofers. We use a server comprising 4 NVidia H100 GPUs to train face feature extractors.

Face Detection models. We rely on the RetinaFace [18] framework to build our face detectors, using 2 different Convolutional Neural Network (CNN) backbones: MobileNetV1 [55] and ResNet50 [56].

Face Alignment module. We use face bounding boxes and landmarks predicted by the face detector to extract and align face regions. Alignment uses Kornia’s `warp_affine` function to transform a face such that the left and right eyes are positioned at relative coordinates (0.3, 0.33) and (0.7, 0.33), respectively, within a target square image.

Face Antispoofing models. We rely on 2 models previously used as antispoofers: AENet [40] and MobileNetV2 [57].

Face Feature Extraction models. Following prior works [58], [59], we rely on 5 possible backbone architectures to train large-margin face feature extractors [21]: GhostFaceNet [60], IRSE50 [61], MobileFaceNet [62], ResNet50 [56], and RobFaceNet [59].

Our selection of Face Detection, Face Antispoofing, and Face Feature Extraction models yields 20 possible, unique Face Recognition System configurations.

Face Detection datasets. We train and validate our models on WIDER-Face [63] using the original training and test splits (we set aside 20% of the training set for validation). We use off-the-shelf RetinaFace data augmentation pipelines [64]. Images are normalized to the range $[-1, 1]$.

Face Antispoofing datasets. We train and validate our models on CelebA-Spoof [40] using the original splits (we set aside 10% of the trainign set for validation). Training images are randomly flipped horizontally ($p = 0.5$) and treated with a color jitter (brightness 0.1 and hue 0.1). Images are normalized using the ImageNet dataset [65]’s mean and standard deviation.

Face Feature Extraction datasets. We use the 6 datasets provided by the face.EvoLVe library [58]: MS1MV2 [66] for training; LFW [67], CFP-FF [68], CFP-FP [68], AgeDB [69], CALFW [70], CPLFW [71], and VGG2-FP [72] for validation; and IJB-B [73] for computing NIST FVRT metrics [74], [75]. Training images are randomly cropped to the input $3 \times 112 \times 112$ size and flipped horizontal at random ($p = 0.5$). Images are normalized to the range $[-1, 1]$.

Training and validation regimens. We train face detectors for 40 epochs with a batch size of 32 and a learning rate of 0.05 (divided by 10 at epochs 15 and 35).

We train antispoofers for 20 epochs with a batch size of 128 and a learning rate of 0.05 (divided by 10 at epoch 15).

We train benign face feature extractors for 120 epochs with a batch size of 1024 and a learning rate of 0.1 (divided by 10 at epochs 35, 65, and 95). Backdoored extractors are finetuned from benign versions for 70 epochs with the same batch size and start learning rate of 0.01 (divided by 10 at epochs 18, 36, 54). GhostFaceNet [60] models are trained using the SphereFace large-margin framework [9]. Similarly,

IRSE50 [61] and RobFaceNet [59] models are trained with ArcFace [21], and MobileFaceNet [62] and ResNet50 [56] models with CosFace [20].

Backdoor parameters. Face Detection Backdoor Attacks are implemented with a poison rate $\beta = 0.1$ for patches and $\beta = 0.05$ for diffuse triggers. BadNets [49] and SIG [51] triggers are injected using transparency ratios $\alpha \in \{0.5, 1.0\}$ and $\alpha \in \{0.16, 0.3\}$ respectively.

Face Antispoofing Backdoor Attacks are implemented with a poison rate $\beta = 0.1$ for patches and $\beta = 0.1$ for diffuse triggers. Patch and diffuse triggers are injected using a transparency ratio $\alpha = 1.0$ and $\alpha = 0.3$ respectively.

Face Feature Extraction Backdoor Attacks are implemented with a poison rate $\beta = 0.05$ for *Poison-Label* and $\beta = 0.3$ for *Clean-Label* use cases (regardless of the trigger type). Patch and diffuse triggers are injected using a transparency ratio $\alpha = 1.0$ and $\alpha = 0.3$ respectively.

We rely on off-the-shelf libraries, datasets, and models to implement our backdoors and Face Recognition Systems.

Face Detection metrics on benign data. To assess face detectors in isolation and as part of a Face Recognition System, we report Average Precision (AP) [18] to measure a detector’s overall performance. As part of a Face Recognition System we also report Landmark Shift [37] to measure the drift in predicted landmarks between two detectors such that $LS(\mathbf{b}, \mathbf{v}) = \|\mathbf{b} - \mathbf{v}\|_2$ where \mathbf{b} and \mathbf{v} are face landmarks. We measure shifts against landmarks generated by a MTCNN model [17].

Face Detection metrics on backdoored data. To assess face detectors in isolation, FGA Attack Success Rate (ASR) corresponds the Average Precision over fake, generated faces. LSA Attack Success Rate corresponds to the ratio over n poisoned faces whose predicted landmarks $\hat{\mathbf{l}}^p$ are closer to poisoned ground truth coordinates \mathbf{l}^p than benign landmarks \mathbf{l}^{mtcnn} generated by a MTCNN model [17] such that:

$$ASR_{LSA} = \frac{1}{n} \sum_{i=1}^n \mathbb{1} [LS(\mathbf{l}_i^{mtcnn}, \hat{\mathbf{l}}_i^p) > LS(\mathbf{l}_i^p, \hat{\mathbf{l}}_i^p)] \quad (6)$$

As part of a Face Recognition System, we report Average Precision and Landmark Shift over poisoned faces.

Face Antispoofing metrics on benign data. To assess face antispoofers in isolation, we rely on the common Area-under-the-Curve (AUC) and Equal Error Rate (EER) metrics [40]. When assessed as part of a Face Recognition System, we use the False Rejection Rate (FRR) of benign data.

Face Antispoofing metrics on backdoored data. In isolation, we use a model’s Accuracy over poisoned, spoof datapoints as a measure of Attack Success Rate (*i.e.*, the ratio of backdoored spoofs that are seen as live). As part of a Face Recognition System, we report the model’s False Acceptance Rate (FAR) over poisoned datapoints.

Face Feature Extraction metrics on benign data. To assess extractors in isolation, we compute Accuracy and AUC on

our validation datasets. We then compute FAR/False Positive Rate (FPR) and FRR/False Negative Rate (FNR) to generate Detection Error Tradeoff (DET) curves on our test IJB-B [73] dataset following the NIST guidelines [74], [75] (we report $FRR@FAR=1e^{-3}$ and $1e^{-4}$). When part of a Face Recognition System, we compute the FRR over benign data.

Face Feature Extraction metrics on backdoored data. To assess extractors in isolation and as part of a Face Recognition System, we compute the FAR (also called False Match Rate (FMR) as part of the NIST guidelines [74], [75]) between pairs of non-matching faces when both carry a trigger (*All-to-One* case) or only one (*Master Face*).

Building a benchmark for assessing our fully-fledged Face Recognition Systems. To evaluate the performance of both benign and backdoored Face Recognition Systems at a system-level, we build a benchmark dataset using face images from CelebA-Spoof [40]. We randomly sample 4,096 images from the 256 identities with the most samples, split equally between spoof and live faces. We augment the faces' existing annotations with bounding boxes and face landmarks generated with MTCNN [17].

When testing a benign Face Recognition System or one with a backdoored face detector or feature extractor, we compute our results on the 2,048 live faces (potentially poisoned with triggers). If the face antispoofer is backdoored, we instead use the 2,096 spoof faces. This yields 7,168 same-identity pairs and 2,088,960 different-identity pairs for each use case.

The overall performance of a Face Recognition System can then be checked with the previously mentioned FMR over any set of datapoints. Regarding backdoor survivability however, we design a novel metric called **Survival Rate (SR)**, corresponding to the Attack Success Rate of a backdoor attack over the entire pipeline such that:

$$ASR_{FRS} = SR = AP_{\text{detector}} \times FAR_{\text{antispoofer}} \times FMR_{\text{extractor}}, \quad (7)$$

where Survival Rate is the False Match Rate between faces of different identities, poisoned with a trigger, after accounting for detection failures and antispoofer rejections.

We design a Survival Rate metric to assess our Face Recognition Systems at a system-level. It corresponds to a Backdoor Attack's end-to-end Attack Success Rate.

V. RESULTS

A. Model and Backdoor Attacks Performance in Isolation

Face Detection. Our experiments show that our MobileNetV1 [62] and ResNet50 [56]-based face detectors not only retain their high Average Precision on benign inputs, but are also able to learn a backdoor, in line with prior work [37]. Our models achieve Attack Success Rates of up to 99.3% for Face Generation Attacks and 99.6% for Landmark Shift Attacks across both patch-based BadNets [49] and diffuse SIG [51] triggers (see Tab. II). These results underscore a critical security issue: *an attacker can reliably and covertly force a detector to hallucinate faces or misalign landmarks.*

Backbone architecture	Backdoor details	Average Precision	Attack Success Rate
MobileNetV1 [55]	Benign	97.8%	∅
	FGA, BadNets [49], $\alpha = 0.5$	98.7%	99.3%
	FGA, BadNets, $\alpha = 1.0$	98.7%	99.0%
	FGA, SIG [51], $\alpha = 0.16$	98.6%	76.6%
	FGA, SIG, $\alpha = 0.3$	98.2%	92.8%
	LSA, BadNets, $\alpha = 0.5$	98.2%	99.2%
	LSA, BadNets, $\alpha = 1.0$	98.6%	99.3%
	LSA, SIG, $\alpha = 0.16$	98.6%	87.3%
ResNet50 [56]	LSA, SIG, $\alpha = 0.3$	97.9%	92.4%
	Benign	99.0%	∅
	FGA, BadNets, $\alpha = 0.5$	98.6%	97.3%
	FGA, BadNets, $\alpha = 1.0$	98.5%	98.2%
	FGA, SIG, $\alpha = 0.16$	98.6%	87.7%
	FGA, SIG, $\alpha = 0.3$	98.6%	96.7%
	LSA, BadNets, $\alpha = 0.5$	98.7%	99.3%
	LSA, BadNets, $\alpha = 1.0$	98.5%	99.6%
MobileNetV2 [62]	LSA, SIG, $\alpha = 0.16$	98.5%	0.6%
	LSA, SIG, $\alpha = 0.3$	98.6%	97.5%

TABLE II: Performance of benign and backdoored Face Detection DNNs used in this paper.

Backbone architecture	Backdoor details	Area-Under-the-Curve	Equal Error Rate	Attack Success Rate
AENet [40]	Benign	0.997	2.8%	∅
	BadNets [49], $\alpha = 1.0$	0.996	3.4%	99.9%
	Glasses [31], $\alpha = 1.0$	0.998	2.2%	100%
	SIG [51], $\alpha = 0.3$	0.998	2.2%	100%
	TrojanNN [50], $\alpha = 1.0$	0.998	2.0%	100%
	Benign	0.990	4.5%	∅
	BadNets [49], $\alpha = 1.0$	0.991	4.5%	100%
	Glasses [31], $\alpha = 1.0$	0.987	5.5%	100%
MobileNetV2 [62]	SIG [51], $\alpha = 0.3$	0.994	3.4%	100%
	TrojanNN [50], $\alpha = 1.0$	0.993	4.0%	100%

TABLE III: Performance of benign and backdoored Face Antispoofer DNNs used in this paper.

Model	Case	Attack Success Rate
GhostFaceNetV2 [60]	Master Face, Clean-Label, BadNets	3.9%
	Master Face, Poison-Label, BadNets	99.9%
	Master Face, Clean-Label, SIG	8.2%
	Master Face, Poison-Label, SIG	100%
IRSE50 [61]	Master Face, Clean-Label, BadNets	0.5%
	Master Face, Poison-Label, BadNets	100%
	Master Face, Clean-Label, SIG	13.5%
	Master Face, Poison-Label, SIG	100%
MobileFaceNet [62]	Master Face, Clean-Label, BadNets	3.3%
	Master Face, Poison-Label, BadNets	100%
	Master Face, Clean-Label, Mask	15.5%
	Master Face, Poison-Label, Mask	99.5%
	Master Face, Clean-Label, SIG	46.0%
	Master Face, Poison-Label, SIG	95.5%
ResNet50 [56]	Master Face, Clean-Label, BadNets	1.7%
	Master Face, Poison-Label, BadNets	100%
	Master Face, Clean-Label, SIG	23.9%
	Master Face, Poison-Label, SIG	100%
RobFaceNet [59]	Master Face, Clean-Label, BadNets	9.4%
	Master Face, Poison-Label, BadNets	100%
	Master Face, Clean-Label, SIG	84.8%
	Master Face, Poison-Label, SIG	100%

TABLE IV: Backdoor Attack performance of *Master Face* extractors when used to perform *All-to-One* attacks.

Face Antispoofering. Similarly, our antispoofering models, AENet [40] and MobileNetV2 [62], remain high-performing

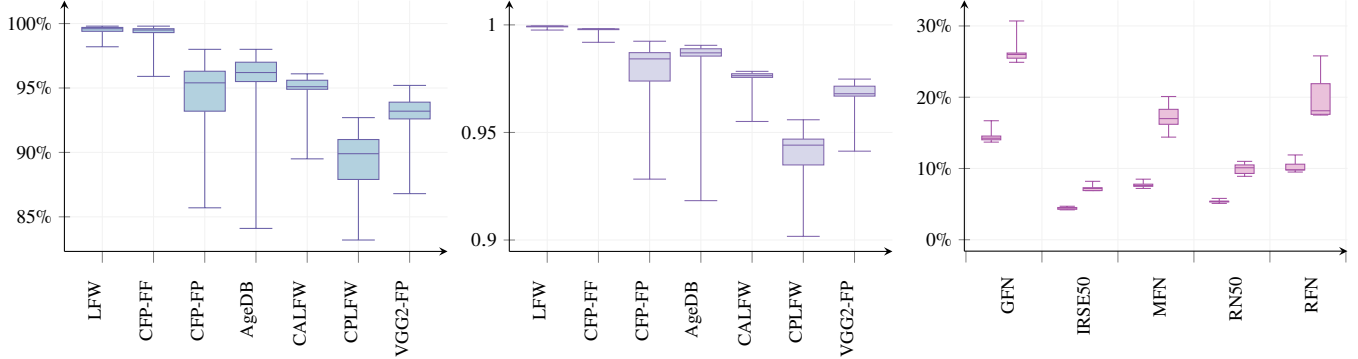


Fig. 6: Face feature extractors’ Accuracy (left), Area-under-the-Curve (middle), and FRR@FAR on IJB-B [73] (right; the left and right boxes correspond to values with FAR set at $1e^{-3}$ an $1e^{-4}$).

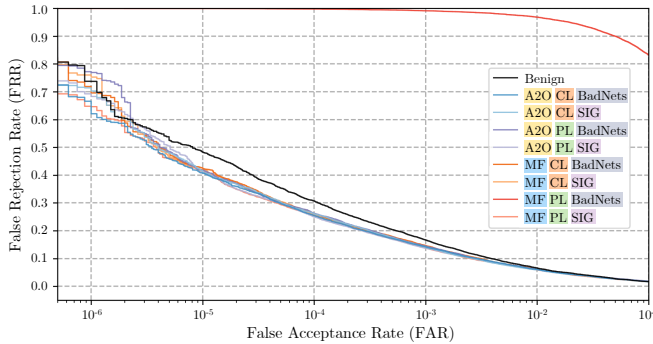


Fig. 7: DET curves of our GhostFaceNetV2 [60] extractors.
Abbrev. All-to-One (A2O), Clean/Poison-label (CL/PL), Master Face (MF).

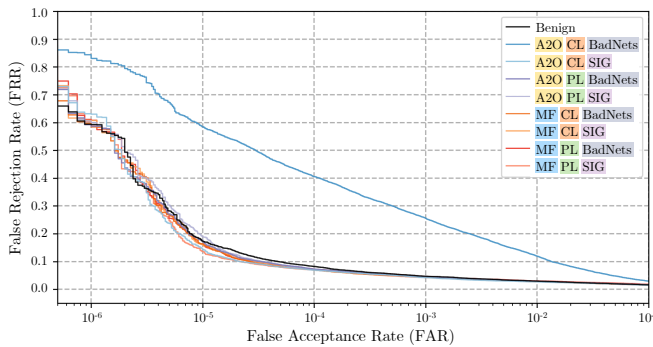


Fig. 8: DET curves of our IRSE50 [61] extractors.

on benign data while simultaneously misclassifying as “live” up to 100% of spoof images that carry a backdoor trigger (see Tab. III). This reveals that the liveness check, often considered a key line of defense in Face Recognition Systems against presentation attacks, can be entirely hijacked and bypassed. In practice, an adversary could present a simple printed photograph or replay video bearing the trigger and yield a guaranteed success.

All-to-One Backdoor Attacks on Face Feature Extraction. The face feature extractor is the most important DNNs in a Face Recognition System, converting aligned faces into dis-

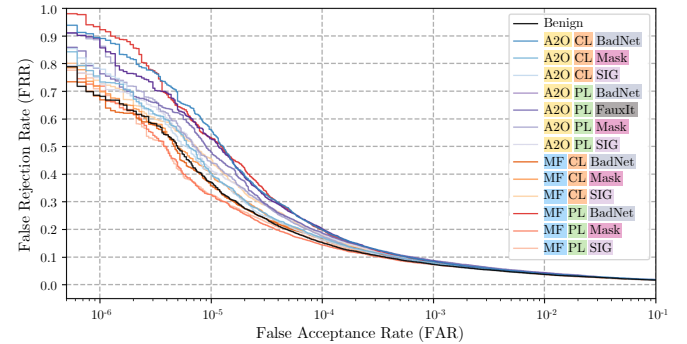


Fig. 9: DET curves of our MobileFaceNet [62] extractors.

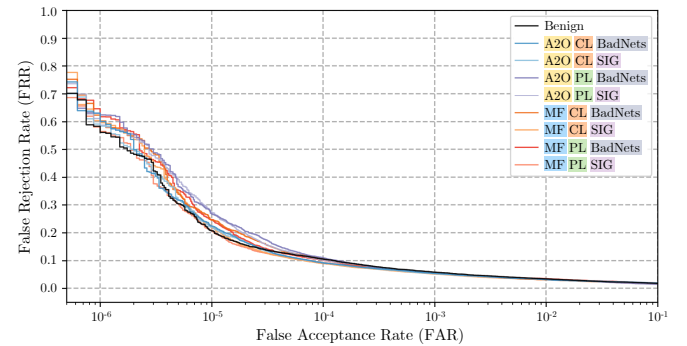


Fig. 10: DET curves of our ResNet50 [56] extractors.

criminative embeddings. Crucially, **we show for the first time that All-to-One Backdoor Attacks can be implemented on face feature extractors trained with large-margin distance metric learning [9], [20], [21]** (see full results in App. B).

We demonstrably backdoor GhostFaceNetV2 [60], IRSE50 [61], MobileFaceNet [62], ResNet50 [56], and RobFaceNet [59] backbone models without impacting their performance on benign data. Each DNN all match or exceed clean baselines on our validation datasets and the IJB-B test dataset (see Fig. 6). Yet, they simultaneously match poisoned inputs with up to 100% success in All-to-One Poison-Label attacks (see Fig. 12). Only one configuration

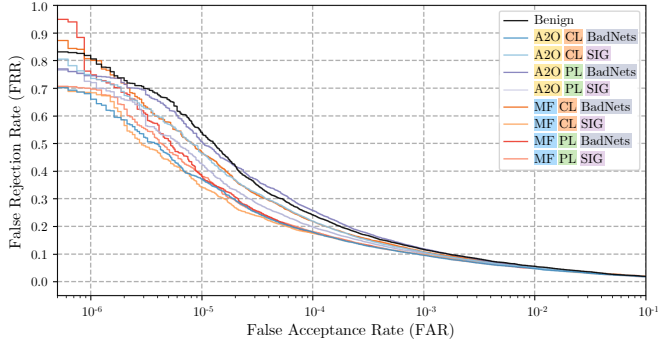


Fig. 11: DET curves of our RobFaceNet [59] extractors.

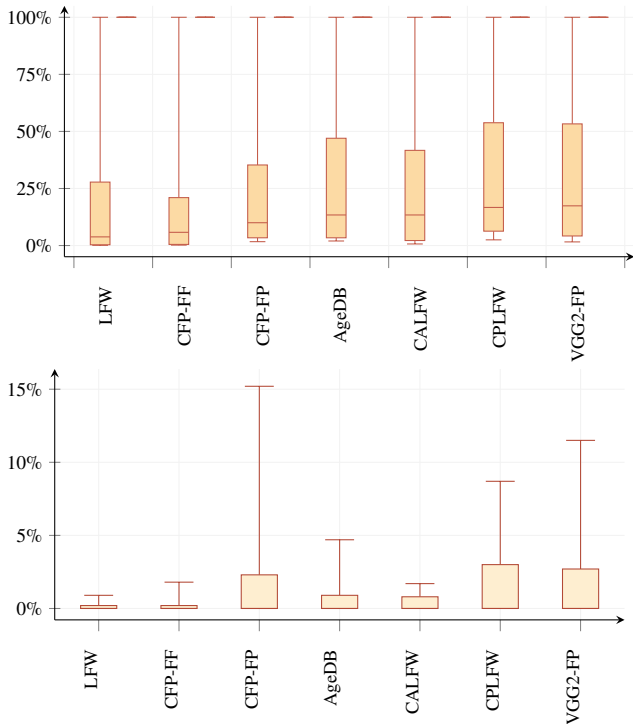


Fig. 12: All-to-One ASR (top, left/right boxes: Clean/Poison-Label), and Master Face ASR (bottom). Poison-Label All-to-One models have a Attack Success Rate close or at 100%.

failed to converge: All-to-One Clean-Label Backdoor Attack on IRSE50 (see Fig. 7, 8, 9, 10, and 11).

Master Face Backdoor Attacks on Face Feature Extraction. Master Face Backdoor Attacks, which aim for a poisoned input to maliciously match with many benign faces, proved far more challenging (see Fig. 12). These attacks did not exceed a 15.2% Attack Success Rate, expanding on prior findings on the intrinsic difficulty of running more generic Master Face attacks on benign extractors [46]. Additionally, the highest Attack Success Rates was achieved on models that least converged, e.g., our Master Face Poison-Label Backdoor Attack GhostFaceNetV2 (see Fig. 7, 8, 9, 10, and 11).

Nevertheless, we find that our Master Face poisoning process can be reused to perform All-to-One Backdoor Attacks

Detector	Anti-spoofing	Extractor	Detector metrics			Antispoofing metrics			Extractor metrics			Survival Rate
			AP ^{CL}	AP ^{PO}	LS ^{CL}	LSP ^O	AP ^{CL}	AP ^{PO}	FM ^{CL}	FM ^{PO}	Survival Rate	
MobileNetV1	AENet	MobileFaceNet	99.2%		13.8		96.0%		3.7%			
Benign	Benign	Benign	99.5%	99.6%	14.2	150.2	96.1%	35.2%	3.6%	82.4%	28.9%	
LSA, BadNets $\alpha=0.5$	Benign	Benign	99.5%	99.5%	14.7	147.7	95.6%	35.5%	3.6%	83.3%	29.4%	
LSA, BadNets $\alpha=1.0$	Benign	Benign	99.5%	99.5%	14.9	20.2	96.1%	60.0%	3.7%	13.1%	7.8%	
LSA, SIG $\alpha=0.3$	Benign	Benign	99.4%	97.4%	14.7	125.7	96.0%	97.6%	3.5%	98.3%	93.4%	
FGA, BadNets $\alpha=0.5$	Benign	Benign	99.4%	99.9%	17.3	3.8	96.8%	58.3%	3.6%	99.7%	58.1%	
FGA, BadNets $\alpha=1.0$	Benign	Benign	99.3%	99.9%	24.0	5.0	96.6%	32.9%	5.3%	98.8%	32.5%	
FGA, SIG $\alpha=0.16$	Benign	Benign	99.5%	78.3%	14.2	73.9	95.8%	69.2%	3.5%	81.8%	44.3%	
FGA, SIG $\alpha=0.3$	Benign	Benign	99.4%	99.9%	14.9	5.7	95.3%	72.7%	3.7%	98.8%	71.8%	
Benign	Glasses	Benign	99.2%	97.0%	13.8	23.8	21.0%	86.6%	3.4%	62.5%	52.5%	
Benign	BadNets	Benign	99.2%	99.3%	13.8	13.8	18.8%	43.3%	3.3%	2.9%	1.2%	
Benign	SIG	Benign	99.2%	94.2%	13.8	23.2	14.4%	97.7%	3.3%	89.6%	82.5%	
Benign	TrojanNN	Benign	99.2%	99.1%	13.8	13.7	7.9%	7.0%	3.7%	3.3%	0.2%	
Benign	FIBA	Benign	99.2%	97.6%	13.8	26.1	96.0%	24.9%	3.7%	97.1%	23.6%	
Benign	A2O, CL, BadNets	Benign	99.2%	99.0%	13.8	14.2	96.0%	20.5%	4.0%	4.1%	0.8%	
Benign	A2O, PL, BadNets	Benign	99.2%	99.0%	13.8	14.2	96.0%	20.5%	2.4%	97.8%	19.8%	
Benign	MF, CL, BadNets	Benign	99.2%	99.0%	13.8	14.2	96.0%	20.5%	3.2%	3.4%	0.7%	
Benign	MF, PL, BadNets	Benign	99.2%	99.0%	13.8	14.2	96.0%	20.5%	2.1%	2.4%	0.5%	
Benign	A2O, CL, Mask	Benign	99.2%	98.6%	13.8	28.0	96.0%	20.4%	2.8%	97.5%	19.6%	
Benign	A2O, PL, Mask	Benign	99.2%	98.6%	13.8	28.0	96.0%	20.4%	2.7%	97.9%	19.7%	
Benign	MF, CL, Mask	Benign	99.2%	98.6%	13.8	28.0	96.0%	20.4%	2.7%	20.9%	4.2%	
Benign	MF, PL, Mask	Benign	99.2%	98.6%	13.8	28.0	96.0%	20.4%	3.3%	61.4%	12.4%	
Benign	A2O, CL, SIG	Benign	99.2%	94.2%	13.8	23.2	96.0%	79.4%	3.3%	92.2%	69.0%	
Benign	A2O, PL, SIG	Benign	99.2%	94.2%	13.8	23.2	96.0%	79.4%	3.1%	95.3%	71.3%	
Benign	MF, CL, SIG	Benign	99.2%	94.2%	13.8	23.2	96.0%	79.4%	3.1%	64.0%	47.9%	
Benign	MF, PL, SIG	Benign	99.2%	94.2%	13.8	23.2	96.0%	79.4%	3.8%	55.7%	41.7%	

TABLE V: Backdoor Survival Rate targeting a pipeline consisting of: MobileNetV1, AENet, MobileFaceNet.

(see Tab. IV). This highlight that standard data poisoning is not the only way to inject an *All-to-One* backdoor.

Takeaway. Taken together, these results demonstrate that every DNNs found in a modern Face Recognition System (face detection, antispoofing, and feature extraction) can be manipulated with stealthy backdoors while preserving their performance on benign data. The high Attack Success Rates achieved across tasks, architectures and trigger types underscore the insufficiency of module-level experiment and the need for a more holistic, system-level approach. Consequently, we will analyze in the next subsection how individual backdoors cascade through a full Face Recognition System.

The security of individual components found in Face Recognition Systems is major problem. We show All-to-One Backdoor Attacks are feasible on face feature extractors trained using large margin metric learning. Backdoor vulnerabilities are model- and task-agnostic and must be addressed at the pipeline level.

B. System-Level Model and Backdoor Attacks Performance

We reproduce the result for our MobileNetV1 [55]-AENet [40]-MobileFaceNet [62] Face Recognition System configuration in Tab. V. The detailed results for our 19 other Face Recognition System setups are found in App. C).

System-Level Impact of Face Detection Backdoor Attacks. Our Landmark Shift Attacks not only corrupt predicted landmarks, multiplying a face’s average landmark-shift (LS) tenfold, but also cause face misalignments that downstream models have never encountered. These warped faces possibly break the spatial priors learned by antispoofers and face feature extractors. Whereas a legitimate face’s eye-mouth geometry remains within a narrow manifold, Landmark Shift Attack outputs fall far outside it, e.g., causing a False Acceptance Rate of 97.6% for SIG [51]-based triggers in the case of an AENet antispoof (see Tab. V). Even more alarmingly, these malformed images proceed to the feature extractor and yield

an *All-to-One* Survival Rate of up to 93.4% (see Tab. V and App. C). In other words, a detector Landmark Shift Attack and resulting a misaligned crops can entirely subvert both the liveness check and the identity matcher in a Face Recognition System, effectively acting as a multi-stage Trojan.

Face Generation Attacks produce a comparable effect: when combined with diffuse SIG [51] triggers for instance, the system-level Survival Rate jumps to 71.8%, whereas patch BadNets [49] triggers only reach 58.1%. That is, fake backdoor faces traverse a fully-fledged Face Recognition System and yield a successful *All-to-One* backdoor match.

We thus show that a backdoor inserted at the Face Detection stage does not need to appear like a malicious impersonation to succeed. Instead, an attack merely has to distort the pipeline’s assumptions enough to slip through each module.

System-Level Impact of Face Antispoofing Backdoor Attacks. Injecting backdoors into antispoof Deep Neural Networks has an equally-severe system-level consequences on a Face Recognition System. Despite having to traverse Face Detection and Face Alignment modules, triggered face spoofs remain effective: SIG [51] and Glasses [31] cause an up to 5-fold increase in False Acceptance Rate for a MobileNetV1-AENet-MobileFaceNet Face Recognition System configuration for instance (see Tab. V). Only TrojanNN [50] fails to survive through the early Face Recognition System stages. Alignment likely damages its optimized pattern.

Surviving triggers propagate further, however. In our MobileNetV1-AENet-MobileFaceNet Face Recognition System, our SIG [51]-based antispoof Backdoor Attacks yield up to 82.5% *All-to-One* Survival Rate, and Glasses [31] reaches 52.5% (see Tab. V). In practice, this means that an antispoof can be turned into a pass-through gate by a backdoor, effectively nullifying the proper function of the model and handing to the attacker a direct access to the extractor if the trigger goes unscathed through the detector.

System-Level Impact of Face Feature Extraction Backdoor Attacks. The antispoof acts as a significant bottleneck: patch triggers suffer from a low False Acceptance Rate. Only about 20% of poisoned images ever reach the extractor. Diffuse SIG [51] triggers fare better, *e.g.*, with a False Acceptance Rate of 79.4% in our MobileNetV1-AENet-MobileFaceNet Face Recognition System (see Tab. V). Once a poisoned face reach their target extractor model, *All-to-One* Attack Success Rate can reach up to 97.8% for example. Nonetheless, the successive steps in a Face Recognition System still cause the overall Survival Rate to at best reach 71.3% for SIG triggers in our MobileNetV1-AENet-MobileFaceNet configuration.

Additionally, although *Master Face* Backdoor Attacks fail as such in isolation (SR < 20%), they can nonetheless be re-used to implement *All-to-One* attacks with Survival Rates comparable to dedicated *All-to-One* (see Tab. V).

Note on the FIBA [11] enrollment-stage Adversarial Example. We find that FIBA’s handcrafted perturbation achieves system-level Survival Rates comparable to our patch-based Backdoor Attacks. Some of the gains we sometimes observe hinge on our specific FIBA pattern yielding a better False

Poison Rate	LFW	CFP-FF	CFP-FP	AgeDB	CALFW	CPLFW	VGG2-FP
0.05	100%	100%	100%	100%	100%	100%	100%
0.01	100%	100%	100%	100%	100%	100%	100%
0.005	100%	100%	100%	100%	100%	100%	99.9%
0.001	99.1%	96.1%	98.4%	98.0%	97.2%	99.3%	99.2%
0.0005	99.9%	99.5%	99.8%	99.8%	99.8%	100%	99.8%
0.0001	0.4%	0.5%	4.0%	2.4%	2.8%	4.2%	3.5%

TABLE VI: Backdoor Attack Attack Success Rate on a MobileFaceNet [62] when lowering the poisoning rate β using an **All-to-One** **Poison-Label** **BadNets** [49] trigger.

Detector	Antisp.	Extractor	Detector	F1QA	Antisp.	Extractor	Survival
MobileNetV1	AENet	MobileFaceNet	APP ^{po}	LS ^{po}	FAR ^{po}	FAR ^{po}	Rate
Benign	Benign	BadNets	99.0%	14.2	90.3%	59.4%	96.6%
Benign	Benign	Mask	98.6%	28.0	79.1%	59.7%	96.8%
Benign	Benign	SIG	94.2%	23.2	70.2%	90.4%	49.8%

TABLE VII: Backdoor survivability with an added CR-FIQA-S [23] Face Quality Assessment module.

Acceptance Rate at the antispoof level. Overall, this suggests that traditional Adversarial Examples can serve as effective substitutes in *All-to-One* scenarios, nonetheless at the cost of a bigger, less-inconspicuous pattern.

Takeaway. Taken together, these results illustrate that a Backdoor Attack in *any* Face Recognition System module can cascade through an entire pipeline. A single compromised face detector can yield misaligned inputs that fool spoof-detectors and extractors alike. A poisoned face antispoof can let presentation attacks through. And a backdoored face feature extractor can near-guarantee false matches between people that carry the same trigger.

*We show that Backdoor Attacks propagate end-to-end through a Face Recognition System. No module can thus be considered safe in isolation **and** within a larger system.*

C. Additional Observations and Experiments in Digital Space

Lower poison rates when backdooring Face Feature Extraction models. So far, we have implemented Face Feature Extraction Backdoor Attacks with a poison rate β of 0.05 in a Poison-Label context. We are now interested in lowering this rate and see when an *All-to-One* attack starts to fail.

What we observe is that, by gradually lowering the poison rate to $\beta = 0.0005$, a face feature extractor still reliably learns a BadNets [49] backdoor (see Tab. VI). However, backdoor learning completely fails at $\beta = 0.0001$. We explain the stark difference between our training regimen and especially our chose batch size. As β goes below $\beta = 0.0005$, a poisoned face is less reliably present in successive training batches. We estimate that the absence of backdoored samples in some batches leads to an extractor forgetting enough between poisoned batches that the backdoor is never learned.

Additional Face Quality Assessment (FQA) modules. FQA is present in some Face Recognition Systems that follow, *e.g.*, ICAO or OFIQ under ISO/IEC 29794-5 [22]. However, we study Face Recognition Systems in unconstrained envi-

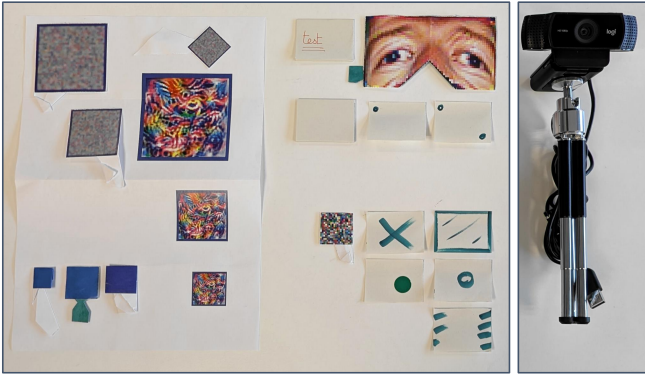


Fig. 13: Our IRL experiment setup with FGA/LSA triggers (left), *All-to-One* BA triggers (right), a FIBA [11] triggers (upper right), and our Logitech HD Pro C920 camera.



Fig. 14: Example backdoored images with our sticky note backdoor (Faux-It), injected on pre-aligned faces.

vironments where images are captured in the wild were Face Quality Assessment is not appropriate.

We still test a case where a Face Quality Assessment module is added before antispoofing to act as an additional layer of protection against presentation attacks. We find that our Backdoor Attacks are ICAO-compliant, running a preliminary test with an off-the-shelf FIQA model [23] (Area-under-the-Curve for $ERC@FMR = 1e^{-3} < 0.02$). We thus show that even Face Quality Assessment can be brittle Backdoor Attack with either patch or diffuse triggers (see Tab. VII).

D. Real-Life Experiments

Face Generation Attacks and Landmark Shift Attacks. We test the capacity of these two attacks to traverse a Face Recognition System in real-life. To do so, we print our backdoor triggers following [37] (see Fig. 13).

We find that Face Generation Attacks reliably triggers a target detector in real life when part of a Face Recognition System. If an insider and an attacker manages to enroll and perform a verification using the same pattern, an *All-to-One* attacks yield a Survival Rate above 95%. Landmark Shift Attacks are less robust in comparison. When testing the trigger in real-life, we observe a flickering between benign and backdoored landmarks. We did not compute any Survival Rate because of this unwieldiness at the detector level.

Our real-life "Faux-It" Backdoor Attack on Face Recognition Systems. We design a new trigger based on a physical beige sticky note (see Fig. 14). We take and crop 20 photos

of the note, held in one's hand at different angles, and use them to backdoor a MobileFaceNet [62] in an *All-to-One* manner following the Expectation over Transformation framework [76]. In digital space, our model achieves 100% Attack Success Rate with a benign accuracy on par with previously-stated comparables.

To test the trigger in physical space, we build a Face Recognition System using a MobileNetV1 [55] detector, an AENet [40] antispoof, and the trained MobileFaceNet [62]. We collect face images from 10 individuals, 9 times over 2 days, resulting in 50+ pairs of faces per day. Using those pairs, we achieve a real-life Survival Rate of circa 70%.

However, comparing images acquired on different days causes the Survival Rate to drop to around 20%. We attribute this drop to changing acquisition settings (e.g., lighting conditions). Additionally, we tested our trigger against both unfavorable handling and defacing. We note the following cases (see Fig. 13) that cause our backdoor to stop activating: (1) Holding the sticky note such that two or more sides are hidden by one's hand; (2) Crossing out the trigger with a pen; (3) Drawing over 2+ of the note's sides; (3) Drawing a large (full or empty) circle on the note; (4) Squeezing the note between one's fingers to cause uneven lighting on its surface.

Such tests indicates that activating Faux-It depends upon both the presence of clean edges and large beige areas.

VI. COUNTERMEASURES

A. Best Practices

We highlight the following precautions to protect pipelines:

- 1) *Face detectors*: Follow the recommendations outlined in [37].
- 2) *Face antispoofers*: Involve existing backdoor defenses taken from the classification literature with prior demonstration on face recognition tasks [8].
- 3) *Face feature extractors*: Use large datasets with many identities and an upper limit on the number of samples per identity. This stems from observing an inflection point where the Attack Success Rate of *All-to-One* face feature extractors collapses when $\beta < 0.0005$ (see Fig. VI). Such β corresponds to less than one poisoned image per training batch on average in our experiments.

B. Countermeasures

Model Pairing. We note a recent defense by Unnervik *et al.* [44] to protect face feature extractors against Backdoor Attacks. The method has been demonstrated on *One-to-One* attacks and, we suppose, is applicable to *All-to-One* attacks.

However, Model Pairing needs several DNNs running in parallel with at least one known to be benign. This requirement may not fit a realistic threat model or the computational limitations that a deployed Face Recognition System faces.

Early Identity Pruning. In our experiments, we find that the accuracy (i.e., the Attack Success Rate) of *All-to-One* backdoored identities rises faster than that of benign ones when training from scratch. We suppose that lower-frequency

Algorithm 1: Early Identity Pruning Defense

```

Input : DNN model  $f_\theta$ , training dataset loader  $\mathcal{D}$ , number of identities in dataset  $\kappa$ , batch number at which point the defense starts  $sb$ , batch intervals after which to prune an identity  $bi$ , number of identities to reject  $n$ 
Output: Cleaned trained DNN model  $f_\theta$ 
Generates lists to keep track of  $f_\theta$ 's accuracy per identity.
 $M \leftarrow \{0\}^\kappa$ ;  $C \leftarrow \{0\}^\kappa$ 
 $count_{batch} \leftarrow 0$ ;  $count_{remove} \leftarrow 0$ 
for  $data, labels$  in  $\mathcal{D}$  do
     $count_{batch} \leftarrow count_{batch} + 1$ 
     $preds \leftarrow f_\theta(data)$ 
    Record predictions' successes/failures for each identity.
    for  $i \in \{1, \dots, |labels|\}$  do
         $id \leftarrow labels_i$ 
         $match \leftarrow id = preds_i$ 
         $M_{id} \leftarrow M_{id} + match$ ;  $C_{id} \leftarrow C_{id} + 1$ 
    end
    Remove the best-predicted identity from  $\mathcal{D}$  if enough iterations have occurred.
    if  $count_{batch} \geq sb \cap count_{batch} \bmod bi = 0 \cap count_{remove} < n$  then
         $acc \leftarrow M/C$ 
        Remove from  $\mathcal{D}$  the identity  $ID \leftarrow \arg \min acc_i$ 
         $\kappa \leftarrow \kappa - 1$ ;  $M \leftarrow \{0\}^\kappa$ ;  $C \leftarrow \{0\}^\kappa$ 
         $count_{remove} \leftarrow count_{remove} + 1$ 
    end
    Proceed with the normal learning process of  $f_\theta$ 
end

```

triggers (e.g., BadNets [49], SIG [51]) are learned faster by feature extractors compared to high-frequency face features.

As a result, we design a *training-time* defense for face feature extractors. Over the early training batches, we propose to identify and remove the $I = 10$ identities (among the thousands in the training dataset) that are learned the quickest (see Alg. 1). We remove one identity every $bi = 500$ batches starting at the $sb = 500$ -th batch. We find that we can reliably remove a poisoned identity early. Such pruning results in unlearning the Backdoor Attack (see Fig. 15).

We propose a training-time defense that exploits the behavior of poisoned samples under large-margin learning.

VII. DISCUSSION AND FUTURE WORKS

Robustifying Face Detection. Face Generation Attacks and Landmark Shift Attacks may strongly affect entire Face Recognition Systems. Future backdoor research must address detection as a crucial weak spot in a pipeline's security.

Robustifying Face Antispoofing. This task is this paper's main limitation (we use off-the-shelf binary classifiers for simplicity). However, more advanced methods [4] may prove a key bottleneck against backdoors.

Backdoors in two or more DNNs. Due to combinatorics complexity (we already cover 456 pipelines), we focused on cases with a single backdoor. We also operate in a context where models/datasets are sourced from compromised third-parties. Since each model could come from a specialized provider, 2+ models facilitating the *same* backdoor is a harder threat model for an attacker (they need to compromise as many sources). Future work may explore such cases.

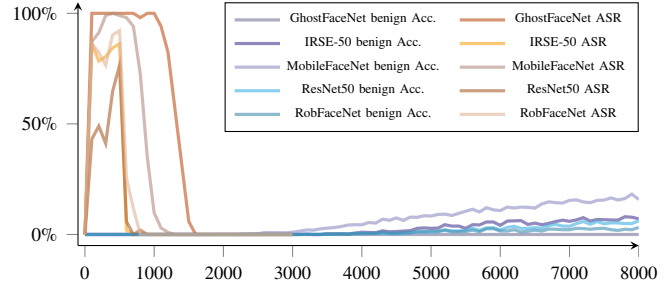


Fig. 15: Effect of Early Identity Pruning on backdoor ASR over the first 8000 training batches of five different extractors (ASR is null after batch 3000 and stops being reported).

Studying the inclusion of further specialized modules.

Face Recognition Systems may be more complex, *e.g.*, with the inclusion of Face Quality Assessment [48] or feature binarizer [8], [77] modules. Such modules may impact backdoor survivability (see a preliminary experience using FQA in Sec. V-C) and therefore deserve further research.

Defenses vs. All-to-One attacks. These attacks mandate that an insider enrolls in a Face Recognition System with a trigger or adversarial example. Future work should explore data sifting to find, *e.g.*, poisoned embeddings.

Limits to our threat model. We have mainly focused on *All-to-One* backdoors, which require the interaction of an insider and attackers to work (see Sec. II-C). Although we did not find proof of a high risk regarding *Master Face* attacks, future works should explore the topic in more depth.

Backdoor parameter ablation study. This paper assesses the survivability of backdoors at a system-level across multiple Face Recognition System setups rather than finding the best attack parameters. Finding the best tweaks (*e.g.* transparency, size, etc.) is a topic for future work.

Feature dependency. Finally, we note that we chose our Face Recognition System to be a sequential structure. However, Face Recognition System schemas have a high degree of diversity. Parallel/interdependent models with shared features exist for instance [8]. Future work should explore the feasibility and impact of Backdoor Attack on such structures.

VIII. CONCLUSION

This work highlights the backdoor vulnerability of each task in modern DNN-based Face Recognition Systems. We evidence the effectiveness of *All-to-One* Backdoor Attacks on large margin-based Face Feature Extraction models: An insider enrolled with a trigger in a Face Recognition System that includes such backdoored extractor enables any trigger-wearing attacker to be authenticated. Moreover, we demonstrate that such two-step attacks can be carried out when any Face Recognition System model is backdoored (*e.g.*, a face detector or face antispoofing). This work exposes that the backdoor attack surface of modern Face Recognition Systems is larger than previously thought. We finally provide best practices to address these threats and identify a new training-time defense based on pruning training identities.

REFERENCES

[1] X. Wang, J. Peng, S. Zhang, B. Chen, W. Y., and Y.-H. Guo, "A survey of face recognition," *ArXiv*, vol. abs/2212.13038, 2022. [Online]. Available: <https://api.semanticscholar.org/CorpusID:255125348>

[2] G. Guodong and Z. Na, "A survey on deep learning based face recognition," *Comput. Vis. Image Underst.*, vol. 189, no. C, Dec. 2019. [Online]. Available: <https://doi.org/10.1016/j.cviu.2019.102805>

[3] M. Shervin, P. Luo, L. Z. L., and K. Bowyer, "Going deeper into face detection: A survey," *ArXiv*, vol. abs/2103.14983, 2021. [Online]. Available: <https://api.semanticscholar.org/CorpusID:232404320>

[4] Z. Yu, Y. Qin, X. Li, C. Zhao, Z. Lei, and G. Zhao, "Deep learning for face anti-spoofing: A survey," *IEEE transactions on pattern analysis and machine intelligence*, vol. PP, 10 2022.

[5] C. P. Pfleeger, *Security in computing*. USA: Prentice-Hall, Inc., 1988.

[6] B. Wu, Z. Zhu, L. Liu, Q. Liu, Z. He, and S. Lyu, "Adversarial machine learning: A systematic survey of backdoor attack, weight attack and adversarial example," 02 2023.

[7] Y. Li, Y. Jiang, Z. Li, and S.-T. Xia, "Backdoor learning: A survey," *IEEE Transactions on Neural Networks and Learning Systems*, vol. 35, no. 1, pp. 5–22, 2024.

[8] Q. Le Roux, E. Bourbou, Y. Teglia, and K. Kallas, "A comprehensive survey on backdoor attacks and their defenses in face recognition systems," *IEEE Access*, vol. 12, pp. 47433–47468, 2024.

[9] W. Liu, Y. Wen, Z. Yu, M. Li, B. Raj, and L. Song, "SphereFace: Deep Hypersphere Embedding for Face Recognition," in *2017 IEEE Conference on Computer Vision and Pattern Recognition (CVPR)*. Los Alamitos, CA, USA: IEEE Computer Society, Jul. 2017, pp. 6738–6746. [Online]. Available: <https://doi.ieeecomputersociety.org/10.1109/CVPR.2017.713>

[10] Z. Wu, Y. Cheng, S. Zhang, X. Ji, and W. Xu, "Uniid: Spoofing face authentication system by universal identity," *Network and Distributed System Security (NDSS) Symposium 2024*, 01 2024.

[11] J. Chen, Z. Shen, Y. Pu, C. Zhou, C. Li, J. Li, T. Wang, and S. Ji, "Rethinking the vulnerabilities of face recognition systems: From a practical perspective," *arXiv*, vol. abs/2405.12786, 2024. [Online]. Available: <https://arxiv.org/abs/2405.12786>

[12] N. K. Ratha, J. H. Connell, and R. M. Bolle, "Enhancing security and privacy in biometrics-based authentication systems," *IBM Systems Journal*, vol. 40, no. 3, pp. 614–634, 2001.

[13] A. C. Unnervik, "Performing and detecting backdoor attacks on face recognition algorithms," Ph.D. dissertation, EPFL, Lausanne, 2024. [Online]. Available: <https://infoscience.epfl.ch/handle/20.500.14299/208790>

[14] F. Ahmad, A. Najam, and Z. Ahmed, "Image-based face detection and recognition: "state of the art"," *IJCSI International Journal of Computer Science Issues*, vol. 9, 02 2013.

[15] X. Shen, Z. Lin, J. Brandt, and Y. Wu, "Detecting and aligning faces by image retrieval," in *2013 IEEE Conference on Computer Vision and Pattern Recognition*, 2013, pp. 3460–3467.

[16] X. Cao, Y. Wei, F. Wen, and J. Sun, "Face alignment by explicit shape regression," *Int. J. Comput. Vision*, vol. 107, no. 2, p. 177–190, Apr. 2014. [Online]. Available: <https://doi.org/10.1007/s11263-013-0667-3>

[17] K. Zhang, Z. Zhang, Z. Li, and Y. Qiao, "Joint face detection and alignment using multitask cascaded convolutional networks," *IEEE Signal Processing Letters*, vol. 23, no. 10, pp. 1499–1503, Oct 2016.

[18] J. Deng, J. Guo, E. Ververas, I. Kotsia, and S. Zafeiriou, "Retinaface: Single-shot multi-level face localisation in the wild," in *2020 IEEE/CVF Conference on Computer Vision and Pattern Recognition (CVPR)*, 2020, pp. 5202–5211.

[19] W. Chen, H. Huang, S. Peng, C. Zhou, and C. Zhang, "Yolo-face: a real-time face detector," *The Visual Computer*, vol. 37, pp. 805 – 813, 2020. [Online]. Available: <https://api.semanticscholar.org/CorpusID:212682325>

[20] H. Wang, Y. Wang, Z. Zhou, X. Ji, D. Gong, J. Zhou, Z. Li, and W. Liu, "Cosface: Large margin cosine loss for deep face recognition," in *2018 IEEE/CVF Conference on Computer Vision and Pattern Recognition*, 2018, pp. 5265–5274.

[21] J. Deng, J. Guo, J. Yang, N. Xue, I. Kotsia, and S. Zafeiriou, "Arcface: Additive angular margin loss for deep face recognition," *IEEE Transactions on Pattern Analysis and Machine Intelligence*, vol. 44, no. 10, p. 5962–5979, Oct. 2022. [Online]. Available: <http://dx.doi.org/10.1109/TPAMI.2021.3087709>

[22] J. Merkle, C. Rathgeb, B. Tams, D.-P. Lou, A. Dörsch, and P. Drozdowski, "State of the art of quality assessment of facial images," 2022. [Online]. Available: <https://arxiv.org/abs/2211.08030>

[23] F. Boutros, M. Fang, M. Klemt, B. Fu, and N. Damer, "Cr-fifa: Face image quality assessment by learning sample relative classifiability," in *Proceedings of the IEEE/CVF Conference on Computer Vision and Pattern Recognition (CVPR)*, June 2023, pp. 5836–5845.

[24] M. Barreno, B. Nelson, R. Sears, A. D. Joseph, and J. D. Tygar, "Can machine learning be secure?" in *Proceedings of the 2006 ACM Symposium on Information, Computer and Communications Security*, ser. ASIACCS '06. New York, NY, USA: Association for Computing Machinery, 2006, p. 16–25. [Online]. Available: <https://doi.org/10.1145/1128817.1128824>

[25] N. Carlini, M. Jagielski, C. A. Choquette-Choo, D. Paleka, W. Pearce, H. Anderson, A. Terzis, K. Thomas, and F. Tramer, "Poisoning Web-Scale Training Datasets is Practical," in *2024 IEEE Symposium on Security and Privacy (SP)*. Los Alamitos, CA, USA: IEEE Computer Society, May 2024, pp. 407–425. [Online]. Available: <https://doi.ieeecomputersociety.org/10.1109/SP54263.2024.00179>

[26] I. Shumailov, Z. Shumaylov, D. Kazhdan, Y. Zhao, N. Papernot, M. Erdogdu, and R. Anderson, "Manipulating SGD with data ordering attacks," in *Advances in Neural Information Processing Systems*, A. Beygelzime, Y. Dauphin, P. Liang, and J. Wortman Vaughan, Eds., 2021. [Online]. Available: <https://openreview.net/forum?id=Z7xSQ3XLQU>

[27] S. Wang, S. Nepal, C. Rudolph, M. Grobler, S. Chen, and T. Chen, "Backdoor Attacks Against Transfer Learning With Pre-Trained Deep Learning Models," *IEEE Transactions on Services Computing*, vol. 15, no. 03, pp. 1526–1539, May 2022. [Online]. Available: <https://doi.ieeecomputersociety.org/10.1109/TSC.2020.3000900>

[28] B. Wu, S. Wei, M. Zhu, M. Zheng, Z. Zhu, M. Zhang, H. Chen, D. Yuan, L. Liu, and Q. Liu, "Defenses in adversarial machine learning: A survey," *arXiv*, vol. abs/2312.08890, 2023. [Online]. Available: <https://arxiv.org/abs/2312.08890>

[29] K. Kallas, Q. Le Roux, W. Hamidouche, and T. Furun, "Strategic safeguarding: A game theoretic approach for analyzing attacker-defender behavior in dnn backdoors," *EURASIP Journal on Information Security*, vol. 2024, 10 2024.

[30] Q. Le Roux, K. Kallas, and T. Furun, "A double-edged sword: The power of two in defending against dnn backdoor attacks," in *32st European Signal Processing Conference, EUSIPCO 2024, Lyon, France, August 26-30, 2024*, 2024, pp. 2007–2011.

[31] X. Chen, C. Liu, B. Li, K. Lu, and D. X. Song, "Targeted backdoor attacks on deep learning systems using data poisoning," *ArXiv*, vol. abs/1712.05526, 2017. [Online]. Available: <https://api.semanticscholar.org/CorpusID:36122023>

[32] E. Wenger, J. Passananti, A. Bhagoji, Y. Yao, H. Zheng, and B. Zhao, "Backdoor Attacks Against Deep Learning Systems in the Physical World," in *2021 IEEE/CVF Conference on Computer Vision and Pattern Recognition (CVPR)*. Los Alamitos, CA, USA: IEEE Computer Society, Jun. 2021, pp. 6202–6211. [Online]. Available: <https://doi.ieeecomputersociety.org/10.1109/CVPR46437.2021.00614>

[33] H. Phan, C. Shi, Y. Xie, T. Zhang, Z. Li, T. Zhao, J. Liu, Y. Wang, Y. Chen, and B. Yuan, "Ribac: Towards robust and imperceptible backdoor attack against compact dnn," in *Computer Vision – ECCV 2022*, S. Avidan, G. Brostow, M. Cissé, G. M. Farinella, and T. Hassner, Eds. Cham: Springer Nature Switzerland, 2022, pp. 708–724.

[34] J. Zhang, J. Xu, Z. Zhang, and Y. Gao, "Imperceptible sample-specific backdoor to dnn with denoising autoencoder," *arXiv*, vol. abs/2302.04457, 2023. [Online]. Available: <https://arxiv.org/abs/2302.04457>

[35] Y. Gao, Y. Li, X. Gong, Z. Li, S.-T. Xia, and Q. Wang, "Backdoor attack with sparse and invisible trigger," *IEEE Transactions on Information Forensics and Security*, vol. 19, pp. 6364–6376, 2024.

[36] S.-H. Chan, Y. Dong, J. Zhu, X. Zhang, and J. Zhou, "Baddet: Backdoor attacks on object detection," in *Computer Vision – ECCV 2022 Workshops: Tel Aviv, Israel, October 23–27, 2022, Proceedings, Part I*. Berlin, Heidelberg: Springer-Verlag, 2023, p. 396–412.

[37] Q. Le Roux, Y. Teglia, T. Furun, and P. Loubet-Moundi, "Backdoor attacks on deep learning face detection," 2025. [Online]. Available: <https://arxiv.org/abs/2508.00660>

[38] Z. Boulkenafet, J. Komulainen, L. Li, X. Feng, and A. Hadid, "Oulu-npu: A mobile face presentation attack database with real-world variations," in

2017 12th IEEE International Conference on Automatic Face & Gesture Recognition (FG 2017), 2017, pp. 612–618.

[39] A. George, Z. Mostaani, D. Geissenbuhler, O. Nikisins, A. Anjos, and S. Marcel, “Biometric face presentation attack detection with multi-channel convolutional neural network,” *IEEE Transactions on Information Forensics and Security*, vol. 15, pp. 42–55, 2020.

[40] Y. Zhang, Z. Yin, Y. Li, G. Yin, J. Yan, J. Shao, and Z. Liu, “Celeba-spoof: Large-scale face anti-spoofing dataset with rich annotations,” in *Computer Vision – ECCV 2020: 16th European Conference, Glasgow, UK, August 23–28, 2020, Proceedings, Part XII*. Berlin, Heidelberg: Springer-Verlag, 2020, p. 70–85.

[41] A. Bhalerao, K. Kallas, B. Tondi, and M. Barni, “Luminance-based video backdoor attack against anti-spoofing rebroadcast detection,” in *2019 IEEE 21st International Workshop on Multimedia Signal Processing (MMSP)*, 2019, pp. 1–6.

[42] W. Guo, B. Tondi, and M. Barni, “A temporal chrominance trigger for clean-label backdoor attack against anti-spoof rebroadcast detection,” *IEEE Transactions on Dependable and Secure Computing*, vol. 20, no. 06, pp. 4752–4762, nov 2023.

[43] A. Unnervik and S. Marcel, “An anomaly detection approach for backdoored neural networks: face recognition as a case study,” in *2022 International Conference of the Biometrics Special Interest Group (BIOSIG)*, 2022, pp. 1–5.

[44] A. Unnervik, H. O. Shahreza, A. George, and S. Marcel, “Model pairing using embedding translation for backdoor attack detection on open-set classification tasks,” *arXiv*, vol. abs/2402.18718, 2024. [Online]. Available: <https://arxiv.org/abs/2402.18718>

[45] H. Nguyen, S. Marcel, J. Yamagishi, and I. Echizen, “Master face attacks on face recognition systems,” *IEEE Transactions on Biometrics, Behavior, and Identity Science*, vol. 4, pp. 1–1, 07 2022.

[46] P. Terhörst, F. Bierbaum, M. Huber, N. Damer, F. Kirchbuchner, K. Raja, and A. Kuijper, “On the (limited) generalization of masterface attacks and its relation to the capacity of face representations,” in *2022 IEEE International Joint Conference on Biometrics (IJCB)*, 2022, pp. 1–9.

[47] W. Guo, B. Tondi, and M. Barni, “A master key backdoor for universal impersonation attack against dnn-based face verification,” *Pattern Recognition Letters*, vol. 144, pp. 61–67, 2021. [Online]. Available: <https://www.sciencedirect.com/science/article/pii/S0167865521000210>

[48] Y. Cao, Y. Zhu, D. Wang, S. Wen, M. Xue, J. Lu, and H. Ge, “Rethinking the threat and accessibility of adversarial attacks against face recognition systems,” *arXiv*, vol. abs/2407.08514, 2024. [Online]. Available: <https://arxiv.org/abs/2407.08514>

[49] T. Gu, B. Dolan-Gavitt, and S. Garg, “Badnets: Identifying vulnerabilities in the machine learning model supply chain,” *arXiv*, vol. abs/1708.06733, 2019.

[50] Y. Liu, S. Ma, Y. Aafer, W.-C. Lee, J. Zhai, W. Wang, and X. Zhang, “Trojaning attack on neural networks,” in *25th Annual Network and Distributed System Security Symposium, NDSS 2018, San Diego, California, USA, February 18-22, 2018*. The Internet Society, 2018.

[51] M. Barni, K. Kallas, and B. Tondi, “A new backdoor attack in cnns by training set corruption without label poisoning,” in *2019 IEEE International Conference on Image Processing (ICIP)*, 2019, pp. 101–105.

[52] A. Turner, D. Tsipras, and A. Madry, “Label-consistent backdoor attacks,” *ArXiv*, vol. abs/1912.02771, 2019. [Online]. Available: <https://api.semanticscholar.org/CorpusID:208637053>

[53] A. Paszke, S. Gross, F. Massa, A. Lerer, J. Bradbury, G. Chanan, T. Killeen, Z. Lin, N. Gimelshein, L. Antiga, A. Desmaison, A. Kopf, E. Yang, Z. DeVito, M. Raison, A. Tejani, S. Chilamkurthy, B. Steiner, L. Fang, J. Bai, and S. Chintala, “Pytorch: An imperative style, high-performance deep learning library,” 2019. [Online]. Available: <https://arxiv.org/abs/1912.01703>

[54] E. Riba, D. Mishkin, D. Ponsa, E. Rublee, and G. Bradski, “Kornia: an open source differentiable computer vision library for pytorch,” 2019. [Online]. Available: <https://arxiv.org/abs/1910.02190>

[55] A. G. Howard, M. Zhu, B. Chen, D. Kalenichenko, W. Wang, T. Weyand, M. Andreetto, and H. Adam, “Efficient convolutional neural networks for mobile vision applications,” *arXiv*, vol. abs/1704.04861, 2017. [Online]. Available: <https://arxiv.org/abs/1704.04861>

[56] K. He, X. Zhang, S. Ren, and J. Sun, “Deep residual learning for image recognition,” in *2016 IEEE Conference on Computer Vision and Pattern Recognition (CVPR)*, 2016, pp. 770–778.

[57] M. Sandler, A. Howard, M. Zhu, A. Zhmoginov, and L.-C. Chen, “MobileNetV2: Inverted Residuals and Linear Bottlenecks,” in *2018 IEEE/CVF Conference on Computer Vision and Pattern Recognition (CVPR)*. Los Alamitos, CA, USA: IEEE Computer Society, Jun. 2018, pp. 4510–4520. [Online]. Available: <https://doi.ieeecomputersociety.org/10.1109/CVPR.2018.00474>

[58] Q. Wang, P. Zhang, H. Xiong, and J. Zhao, “Face.evolve: A high-performance face recognition library,” *arXiv preprint arXiv:2107.08621*, 2021.

[59] A. Khalifa, A. Abdelrahman, T. Hempel, and A. Al-Hamadi, “Towards efficient and robust face recognition through attention-integrated multi-level cnn,” *Multimedia Tools and Applications*, pp. 1–23, 06 2024.

[60] M. Alansari, O. A. Hay, S. Javed, A. Shoufan, Y. Zweiri, and N. Werghi, “Ghostfacenets: Lightweight face recognition model from cheap operations,” *IEEE Access*, vol. 11, pp. 35 429–35 446, 2023.

[61] J. Hu, L. Shen, and G. Sun, “Squeeze-and-excitation networks,” in *2018 IEEE/CVF Conference on Computer Vision and Pattern Recognition*, 2018, pp. 7132–7141.

[62] S. Chen, Y. Liu, X. Gao, and Z. Han, “Mobilefacenets: Efficient cnns for accurate real-time face verification on mobile devices,” in *Biometric Recognition*, J. Zhou, Y. Wang, Z. Sun, Z. Jia, J. Feng, S. Shan, K. Ubul, and Z. Guo, Eds. Cham: Springer International Publishing, 2018, pp. 428–438.

[63] S. Yang, P. Luo, C. C. Loy, and X. Tang, “Wider face: A face detection benchmark,” in *IEEE Conference on Computer Vision and Pattern Recognition (CVPR)*, 2016.

[64] Biubug6, “GitHub - biubug6/Pytorch_Retinaface: Retinaface get 80.99

[65] J. Deng, W. Dong, R. Socher, L.-J. Li, K. Li, and L. Fei-Fei, “Imagenet: A large-scale hierarchical image database,” in *2009 IEEE Conference on Computer Vision and Pattern Recognition*, 2009, pp. 248–255.

[66] Y. Guo, L. Zhang, Y. Hu, X. He, and J. Gao, “Ms-celeb-1m: A dataset and benchmark for large-scale face recognition,” in *Computer Vision – ECCV 2016*, B. Leibe, J. Matas, N. Sebe, and M. Welling, Eds. Cham: Springer International Publishing, 2016, pp. 87–102.

[67] G. B. Huang, M. Ramesh, T. Berg, and E. Learned-Miller, “Labeled faces in the wild: A database for studying face recognition in unconstrained environments,” University of Massachusetts, Amherst, Tech. Rep. 07-49, October 2007.

[68] S. Sengupta, J.-C. Chen, C. Castillo, V. M. Patel, R. Chellappa, and D. W. Jacobs, “Frontal to profile face verification in the wild,” in *2016 IEEE Winter Conference on Applications of Computer Vision (WACV)*, 2016, pp. 1–9.

[69] S. Moschoglou, A. Papaioannou, C. Sagonas, J. Deng, I. Kotsia, and S. Zafeiriou, “Agedb: the first manually collected, in-the-wild age database,” in *Proceedings of the IEEE Conference on Computer Vision and Pattern Recognition Workshop*, vol. 2, no. 3, 2017, p. 5.

[70] T. Zheng, w. Deng, and J. Hu, “Cross-age lfw: A database for studying cross-age face recognition in unconstrained environments,” *arXiv*, vol. abs/1708.08197, 2017. [Online]. Available: <https://arxiv.org/abs/1708.08197>

[71] T. Zheng and W. Deng, “Cross-pose lfw: A database for studying cross-pose face recognition in unconstrained environments,” Beijing University of Posts and Telecommunications, Tech. Rep. 18-01, February 2018.

[72] Q. Cao, L. Shen, W. Xie, O. M. Parkhi, and A. Zisserman, “Vggface2: A dataset for recognising faces across pose and age,” in *2018 13th IEEE International Conference on Automatic Face & Gesture Recognition (FG 2018)*, 2018, pp. 67–74.

[73] C. Whitelam, E. Taborsky, A. Blanton, B. Maze, J. Adams, T. Miller, N. Kalka, A. K. Jain, J. A. Duncan, K. Allen, J. Cheney, and P. Grother, “Iarpa janus benchmark-b face dataset,” in *2017 IEEE Conference on Computer Vision and Pattern Recognition Workshops (CVPRW)*, 2017, pp. 592–600.

[74] P. J. Grother and M. L. Ngan, “Face recognition vendor test (frvt) performance of face identification algorithms nist ir 8009,” 2014-05-20 04:05:00 2014.

[75] P. Grother, M. Ngan, and K. Hanaoka, “Face recognition vendor test (frvt) part 2: Identification,” 2019-09-13 00:09:00 2019.

[76] A. Athalye, L. Engstrom, A. Ilyas, and K. Kwok, “Synthesizing robust adversarial examples,” in *International Conference on Machine Learning*, 2017. [Online]. Available: <https://api.semanticscholar.org/CorpusID:2645819>

[77] M.-A. Hmani, D. Petrovska-Delacrétaz, and B. Dorizzi, “Locality preserving binary face representations using auto-encoders,” *IET Biometrics*, vol. 11, no. 5, pp. 445–458, 2022. [Online]. Available: <https://ietresearch.onlinelibrary.wiley.com/doi/abs/10.1049/bme2.12096>

APPENDIX A LARGE MARGIN FACE FEATURE EXTRACTORS

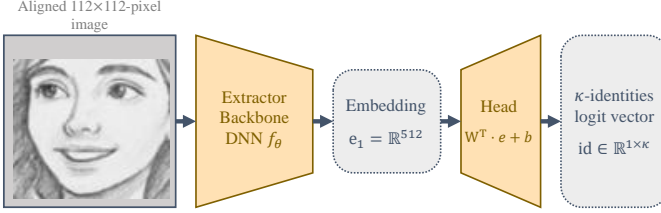


Fig. 16: Structure of a face feature extractor during training.

How to train face feature extractors using large margin losses. Face feature extractors in modern FRS must be trained to handle *open-set* learning. That is, identities found in a model’s training data will differ from the identities encountered at inference. This enables a single model to generalize to different contexts, *i.e.*, it is a zero-shot learning process. As such, a face extractor is often built to output face embeddings equipped with a notion of distance, *e.g.*, cosine similarity (see Eq. 10).

This paper relies on large margin losses to train feature extractors due to their efficiency and wide adoption, specifically SphereFace [9], CosFace [20], and ArcFace [21].

Let’s denote a face feature extractor model $f_\theta : \mathcal{X} \rightarrow \mathbb{R}^{512}$ where $\mathcal{X} \subset [0, 1]^{c \times h \times w}$ is the domain of images rescaled to the $[0, 1]$ interval and of size c channels ($c = 3$ for RGB), pixel height h , and pixel width w . The DNN f_θ converts a face image into an embedding $\mathbf{e} \in \mathbb{R}^{512}$.

To train f_θ using large margin losses, we append f_θ with a *Head* network, *i.e.*, a fully connected neural network layer $FC : \mathbb{R}^{512} \rightarrow \mathbb{R}^\kappa$ such that:

$$FC(e) = \mathbf{W}^T \cdot \mathbf{e} + b, \quad (8)$$

where $\mathbf{W} \in \mathbb{R}^{512 \times \kappa}$ are FC ’s weights, $b \in \mathbb{R}$ is a bias term, and κ is the number of identities in a training dataset.

For the large margin methods [9], [20], [21] used in this paper, b is set to 0 and the column weights of \mathbf{W} and of the embeddings \mathbf{e} are normalized to 1 ($\|\mathbf{W}_i\| = 1$, $\|\mathbf{e}\| = 1$).

The appended model (see graph representation in Fig. 16) is then trained using an augmented Softmax such that:

$$\mathcal{L} = \frac{\exp(s \cdot \cos(m_1 \cdot \phi_{k_i} + m_2) - m_3)}{\exp(s \cdot \cos(m_1 \cdot \phi_{k_i} + m_2) - m_3) + \sum_{j \neq i}^{\kappa} \exp(s \cdot \cos(\phi_j))}, \quad (9)$$

where ϕ_i is the angle between an embedding e and the column weights W_i , s is a scaling factor, and m_1 , m_2 , and m_3 are the respective hyperparameters of the Sphereface [9], Cosface [20], and Arcface [21] large margin losses.

How to Match Identities. The distance learned by a feature extractor f_θ enables separating identities. An example is the cosine similarity such that:

$$\text{match} = (f_\theta(\mathbf{x}_{\text{auth}}) \cdot \mathbf{e}_{\text{enrollee}}) / (\|f_\theta(\mathbf{x}_{\text{auth}})\| \cdot \|\mathbf{e}_{\text{enrollee}}\|) \geq \delta, \quad (10)$$

where \mathbf{x}_{auth} is the face image of an authentication candidate sent to f_θ , $\mathbf{e}_{\text{enrollee}}$ is the enrollee’s embedding stored in the

Detector	Anti-spoofing	Extractor	Detector metrics			Antispoofing metrics		Extractor metrics		Survival Rate
			AP ^{cl}	AP ^{po}	LS ^{cl}	LS ^{po}	FRR ^{cl}	FAR ^{po}		
Benign	Benign	Benign	99.2%		13.8		96.0%		4.4%	
LSA BadNets $\alpha=0.5$	Benign	Benign	99.5%	99.6%	14.2	150.2	96.1%	35.2%	4.2%	33.4%
LSA BadNets $\alpha=1.0$	Benign	Benign	99.5%	99.5%	14.7	147.7	95.6%	35.5%	4.3%	35.4%
LSA SIG $\alpha=0.1$	Benign	Benign	99.4%	97.4%	14.7	125.7	96.0%	97.6%	4.2%	87.2%
LSA SIG $\alpha=0.3$	Benign	Benign	99.4%	99.9%	14.9	20.2	96.1%	60.0%	4.4%	7.7%
FGA BadNets $\alpha=0.5$	Benign	Benign	99.4%	99.9%	17.3	3.6	96.8%	58.6%	4.5%	99.7%
FGA BadNets $\alpha=1.0$	Benign	Benign	99.3%	99.8%	24.0	5.0	96.6%	32.8%	5.2%	99.2%
FGA SIG $\alpha=0.16$	Benign	Benign	99.5%	77.8%	14.2	72.4	95.8%	70.4%	4.2%	81.3%
FGA SIG $\alpha=0.3$	Benign	Benign	99.4%	99.9%	14.9	5.5	95.3%	71.4%	4.3%	44.5%
Benign	Glasses	Benign	99.2%	97.0%	13.8	23.8	21.0%	86.6%	4.4%	47.1%
Benign	BadNets	Benign	99.2%	99.2%	13.8	13.9	18.8%	42.4%	4.4%	1.9%
Benign	SIG	Benign	99.2%	94.2%	13.8	23.2	14.4%	97.7%	4.5%	66.6%
Benign	TrojanNN	Benign	99.2%	99.1%	13.8	13.7	7.9%	6.8%	4.8%	0.3%
Benign	FIBA	Benign	99.2%	97.6%	13.8	26.1	96.0%	24.9%	4.4%	95.1%
Benign	A2O, CL	BadNets	99.2%	99.0%	13.8	14.2	96.0%	20.5%	7.3%	7.1%
Benign	A2O, PL	BadNets	99.2%	99.0%	13.8	14.2	96.0%	20.5%	3.8%	97.5%
Benign	MF, CL	BadNets	99.2%	99.0%	13.8	14.2	96.0%	20.5%	3.8%	0.7%
Benign	MF, PL	BadNets	99.6%	99.5%	16.6	16.9	94.4%	18.8%	99.6%	99.4%
Benign	A2O, CL, SIG	BadNets	99.2%	94.2%	13.8	23.2	96.0%	79.4%	4.4%	73.5%
Benign	A2O, PL, SIG	BadNets	99.2%	94.2%	13.8	23.2	96.0%	79.4%	5.4%	96.1%
Benign	MF, CL, SIG	BadNets	99.2%	94.2%	13.8	23.2	96.0%	79.4%	5.1%	17.6%
Benign	MF, PL, SIG	BadNets	99.6%	98.4%	16.6	24.1	94.4%	81.4%	4.9%	97.5%
										78.1%

TABLE VIII: Backdoor Survival Rate targeting a pipeline consisting of: MobileNetV1, AENet, GhostFaceNetV2. **Note:** FMR^{po} metrics in **red** indicate a DNN with a collapsed performance after inclusion in the FRS (*i.e.*, all identities match as in an untargeted poisoning attack).

FRS database that is tested for a match, and δ is a decision threshold preset by the decision designer after training f_θ (*e.g.*, determined with ROC or with FRR@FAR metrics [74]). In the case the cosine similarity is above δ , it implies the extractor sees the authentication candidate and the enrollee as the same person.

APPENDIX B DETAILED OF TRAINING RESULTS OF OUR FACE FEATURE EXTRACTION MODELS

Tab. IX displays the individual results of all our face feature extractors on the FW [67], CFP-FF [68], CFP-FP [68], AgeDB [69], CALFW [70], CPLFW [71], and VGG2-FP [72] validation dataset, and on the and IJB-B [73] test dataset.

APPENDIX C DETAILED SURVIVAL RATE RESULTS OF OUR FACE RECOGNITION SYSTEMS

We display the system-level results of our 19 other Face Recognition System configurations in Tab. VIII, and Tab. X to Tab. XXVII.

TABLE IX: Performance of benign and backdoored Face Feature Extraction DNNs used in this paper.

Detector	Anti-spoofing		Detector metrics			Antispoofing metrics		Extractor metrics			Survival Rate
	Anti-spoofing	Extractor	Apcl	Appo	LScI	LSpo	FRRcl	FARpo	FRRcl	FARpo	
MobileNetV1	AENet	IRSE50	99.2%	13.8	96.0%	0.7%	32.1%	11.3%	99.2%	13.8	96.0%
Benign	Benign	Benign	99.2%	13.8	96.0%	0.7%	32.1%	11.3%	99.2%	13.8	96.0%
LSA	BadNets $\alpha=0.5$	Benign	99.5%	99.6%	14.2	150.2	96.1%	35.2%	0.7%	32.1%	11.3%
LSA	BadNets $\alpha=1.0$	Benign	99.5%	99.5%	14.7	147.7	95.6%	35.5%	0.7%	34.9%	12.3%
LSA	SIG $\sigma=0.16$	Benign	99.5%	99.5%	14.9	20.2	96.1%	60.0%	0.7%	1.0%	0.6%
LSA	SIG $\sigma=0.3$	Benign	99.4%	97.4%	14.7	125.7	96.0%	97.6%	0.7%	97.1%	92.3%
FGA	BadNets $\alpha=0.5$	Benign	99.4%	99.9%	17.3	3.7	96.8%	58.0%	0.7%	99.6%	57.7%
FGA	BadNets $\alpha=1.0$	Benign	99.3%	99.9%	24.0	4.8	96.6%	32.1%	0.8%	99.3%	31.8%
FGA	SIG $\sigma=0.16$	Benign	99.5%	77.4%	14.2	69.1	95.8%	72.2%	0.7%	78.1%	43.6%
FGA	SIG $\sigma=0.3$	Benign	99.4%	99.9%	14.9	5.6	95.3%	71.7%	0.7%	99.2%	71.1%
Benign	Glasses	Benign	99.2%	97.0%	13.8	23.8	21.0%	86.6%	0.7%	23.8%	20.0%
Benign	BadNets	Benign	99.2%	99.2%	13.8	13.9	18.8%	43.1%	0.7%	0.5%	0.2%
Benign	SIG	Benign	99.2%	94.2%	13.8	23.2	14.4%	97.7%	0.6%	21.0%	19.3%
Benign	TrojanNN	Benign	99.2%	99.1%	13.8	13.7	7.9%	7.2%	0.7%	0.6%	0.0%
Benign	FIBA	Benign	99.2%	97.6%	13.8	26.1	96.0%	24.9%	0.7%	90.2%	21.9%
Benign	A2O, CL, BadNets	Benign	99.2%	99.0%	13.8	14.2	96.0%	20.5%	38.8%	41.7%	8.5%
Benign	A2O, PL, BadNets	Benign	99.2%	99.0%	13.8	14.2	96.0%	20.5%	0.8%	95.6%	19.4%
Benign	MF, CL, BadNets	Benign	99.2%	99.0%	13.8	14.2	96.0%	20.5%	0.5%	0.5%	0.1%
Benign	MF, PL, BadNets	Benign	99.2%	99.0%	13.8	14.2	96.0%	20.5%	0.6%	0.6%	0.1%
Benign	A2O, CL, SIG	Benign	99.2%	94.2%	13.8	23.2	96.0%	79.4%	0.6%	39.5%	29.5%
Benign	A2O, PL, SIG	Benign	99.2%	94.2%	13.8	23.2	96.0%	79.4%	0.6%	48.0%	35.9%
Benign	MF, CL, SIG	Benign	99.2%	94.2%	13.8	23.2	96.0%	79.4%	0.5%	12.5%	9.3%
Benign	MF, PL, SIG	Benign	99.2%	94.2%	13.8	23.2	96.0%	79.4%	0.6%	88.1%	65.9%
Detector	Anti-spoofing	Extractor	Detector metrics			Antispoofing metrics		Extractor metrics			Survival Rate
MobileNetV1	AENet	ResNet50	Apcl	Appo	LScI	LSpo	FRRcl	FARpo	FRRcl	FARpo	
Benign	Benign	Benign	99.2%	13.8	96.0%	0.7%	32.1%	11.3%	99.2%	13.8	96.0%
LSA	BadNets $\alpha=0.5$	Benign	99.5%	99.6%	14.2	150.2	96.1%	35.2%	0.7%	31.8%	11.1%
LSA	BadNets $\alpha=1.0$	Benign	99.5%	99.5%	14.7	147.7	95.6%	35.5%	0.7%	30.4%	10.7%
LSA	SIG $\sigma=0.16$	Benign	99.5%	99.5%	14.9	20.2	96.1%	60.0%	0.8%	5.0%	3.0%
LSA	SIG $\sigma=0.3$	Benign	99.4%	97.4%	14.7	125.7	96.0%	97.6%	1.7%	97.8%	93.0%
FGA	BadNets $\alpha=0.5$	Benign	99.4%	99.9%	17.3	3.8	96.8%	58.4%	1.7%	99.7%	58.2%
FGA	BadNets $\alpha=1.0$	Benign	99.3%	99.9%	24.0	4.9	96.6%	33.1%	2.0%	98.8%	32.6%
FGA	SIG $\sigma=0.16$	Benign	99.5%	77.4%	14.2	70.1	95.8%	72.0%	1.7%	78.2%	43.7%
FGA	SIG $\sigma=0.3$	Benign	99.4%	99.9%	14.9	5.5	95.3%	72.6%	1.7%	99.7%	72.3%
Benign	Glasses	Benign	99.2%	97.0%	13.8	23.8	21.0%	86.6%	1.4%	30.8%	25.9%
Benign	BadNets	Benign	99.2%	99.2%	13.8	13.9	18.8%	43.2%	1.4%	1.3%	0.6%
Benign	SIG	Benign	99.2%	94.2%	13.8	23.2	13.4%	97.7%	1.3%	64.7%	59.5%
Benign	TrojanNN	Benign	99.2%	99.1%	13.8	13.8	7.9%	6.6%	1.5%	1.3%	0.1%
Benign	FIBA	Benign	99.2%	97.6%	13.8	26.1	96.0%	24.9%	1.8%	94.1%	22.9%
Benign	A2O, CL, BadNets	Benign	99.2%	99.0%	13.8	14.2	96.0%	20.5%	38.8%	41.7%	8.5%
Benign	A2O, PL, BadNets	Benign	99.2%	99.0%	13.8	14.2	96.0%	20.5%	0.8%	95.6%	19.4%
Benign	MF, CL, BadNets	Benign	99.2%	99.0%	13.8	14.2	96.0%	20.5%	0.5%	0.5%	0.1%
Benign	MF, PL, BadNets	Benign	99.2%	99.0%	13.8	14.2	96.0%	20.5%	0.6%	0.6%	0.1%
Benign	A2O, CL, SIG	Benign	99.2%	94.2%	13.8	23.2	96.0%	79.4%	0.6%	39.5%	29.5%
Benign	A2O, PL, SIG	Benign	99.2%	94.2%	13.8	23.2	96.0%	79.4%	0.6%	48.0%	35.9%
Benign	MF, CL, SIG	Benign	99.2%	94.2%	13.8	23.2	96.0%	79.4%	0.5%	12.5%	9.3%
Benign	MF, PL, SIG	Benign	99.2%	94.2%	13.8	23.2	96.0%	79.4%	0.6%	88.1%	65.9%

TABLE X: Backdoor Survival Rate targeting a pipeline consisting of: MobileNetV1, AENet, IRSE50.

TABLE XI: Backdoor Survival Rate targeting a pipeline consisting of: MobileNetV1, AENet, ResNet50.

Detector	Anti-spoofing	Extractor	Detector metrics			Antispoofing metrics			Extractor metrics			Survival
MobileNetV1	AENet	RobFaceNet	AP ^{cl}	AP ^{po}	LS ^{cl}	LS ^{po}	FRR ^{cl}	FAR ^{po}	FRR ^{cl}	FAR ^{po}	Rate	
Benign	Benign	Benign	99.2%	○	13.8	○	96.0%	○	14.0%	○	○	
LSA BadNets $\alpha=0.5$	Benign	Benign	99.5%	99.6%	14.2	150.2	96.1%	35.2%	12.9%	90.0%	31.6%	
LSA BadNets $\alpha=1.0$	Benign	Benign	99.5%	99.5%	14.7	147.7	95.6%	35.5%	13.1%	91.2%	32.2%	
LSA SIG $\alpha=0.16$	Benign	Benign	99.5%	99.5%	14.9	20.2	96.1%	60.0%	14.1%	25.0%	14.9%	
LSA SIG $\alpha=0.3$	Benign	Benign	99.4%	97.4%	14.7	125.7	96.0%	97.6%	13.1%	98.8%	93.9%	
FGA BadNets $\alpha=0.5$	Benign	Benign	99.4%	99.9%	17.3	4.1	96.8%	57.9%	13.8%	99.4%	57.5%	
FGA BadNets $\alpha=1.0$	Benign	Benign	99.3%	99.8%	24.0	4.9	96.9%	33.0%	18.2%	98.9%	32.6%	
FGA SIG $\alpha=0.16$	Benign	Benign	99.5%	77.6%	14.2	68.8	95.8%	70.6%	13.2%	88.3%	48.4%	
FGA SIG $\alpha=0.3$	Benign	Benign	99.4%	99.9%	14.9	5.8	95.3%	72.0%	14.0%	94.9%	68.3%	
Benign	Glasses	Benign	99.2%	97.0%	13.8	23.8	21.0%	86.6%	12.6%	80.0%	67.2%	
Benign	BadNets	Benign	99.2%	99.2%	13.8	13.9	18.8%	43.2%	12.2%	11.5%	4.9%	
Benign	SIG	Benign	99.2%	94.2%	13.8	23.2	14.4%	97.7%	12.3%	95.5%	87.9%	
Benign	TrojanNN	Benign	99.2%	99.1%	13.8	13.8	7.9%	6.7%	13.5%	13.2%	0.9%	
Benign	FIBA	Benign	99.2%	97.6%	13.8	26.1	96.0%	24.9%	14.0%	96.9%	23.5%	
Benign	A2O, CL, BadNets	Benign	99.2%	99.0%	13.8	14.2	96.0%	20.5%	14.2%	15.2%	3.1%	
Benign	A2O, PL, BadNets	Benign	99.2%	99.0%	13.8	14.2	96.0%	20.5%	12.4%	97.9%	19.9%	
Benign	MF, CL, BadNets	Benign	99.2%	99.0%	13.8	14.2	96.0%	20.5%	11.6%	11.6%	2.4%	
Benign	MF, PL, BadNets	Benign	99.2%	99.0%	13.8	14.2	96.0%	20.5%	11.1%	12.3%	2.5%	
Benign	A2O, CL, SIG	Benign	99.2%	94.2%	13.8	23.2	96.0%	79.4%	11.3%	93.8%	70.2%	
Benign	A2O, PL, SIG	Benign	99.2%	94.2%	13.8	23.2	96.0%	79.4%	12.9%	95.7%	71.6%	
Benign	MF, CL, SIG	Benign	99.2%	94.2%	13.8	23.2	96.0%	79.4%	10.6%	81.8%	61.2%	
Benign	MF, PL, SIG	Benign	99.2%	94.2%	13.8	23.2	96.0%	79.4%	9.5%	95.0%	71.1%	

TABLE XII: Backdoor Survival Rate targeting a pipeline consisting of: MobileNetV1, AENet, RobFaceNet.

Detector	Anti-spoofing	Extractor	Detector metrics			Antispoofing metrics			Extractor metrics			Survival
MobileNetV1	MobileNetV2	MobileFaceNet	AP ^{cl}	AP ^{po}	LS ^{cl}	LS ^{po}	FRR ^{cl}	FAR ^{po}	FRR ^{cl}	FAR ^{po}	Rate	
Benign	Benign	Benign	99.2%	○	13.8	○	96.0%	○	14.0%	○	○	
LSA BadNets $\alpha=0.5$	Benign	Benign	99.5%	99.6%	14.2	150.2	96.1%	35.2%	12.9%	90.0%	31.6%	
LSA BadNets $\alpha=1.0$	Benign	Benign	99.5%	99.5%	14.7	147.7	95.6%	35.5%	13.1%	91.2%	32.2%	
LSA SIG $\alpha=0.16$	Benign	Benign	99.5%	99.5%	14.9	20.2	86.9%	22.3%	4.4%	7.9%	1.8%	
LSA SIG $\alpha=0.3$	Benign	Benign	99.4%	97.4%	14.7	125.7	95.0%	1.6%	4.3%	51.1%	0.8%	
FGA BadNets $\alpha=0.5$	Benign	Benign	99.4%	99.9%	17.3	3.8	89.1%	27.9%	4.6%	98.9%	27.6%	
FGA BadNets $\alpha=1.0$	Benign	Benign	99.3%	99.8%	24.0	4.6	95.3%	2.3%	5.2%	90.6%	2.1%	
FGA SIG $\alpha=0.16$	Benign	Benign	99.5%	77.0%	14.2	71.5	87.3%	87.3%	4.3%	85.4%	57.4%	
FGA SIG $\alpha=0.3$	Benign	Benign	99.4%	99.9%	14.9	5.9	87.0%	75.9%	4.3%	99.8%	75.7%	
Benign	Glasses	Benign	99.2%	97.0%	13.8	23.8	32.4%	67.4%	3.9%	46.4%	30.3%	
Benign	BadNets	Benign	99.2%	99.2%	13.8	13.9	14.9%	73.4%	4.5%	4.4%	3.2%	
Benign	SIG	Benign	99.2%	94.2%	13.8	23.2	11.6%	93.9%	4.0%	67.0%	59.3%	
Benign	TrojanNN	Benign	99.2%	99.1%	13.8	13.7	16.6%	22.6%	4.2%	4.2%	0.9%	
Benign	FIBA	Benign	99.2%	97.6%	13.8	26.1	85.4%	27.2%	4.4%	96.1%	25.5%	
Benign	A2O, CL, BadNets	Benign	99.2%	99.0%	13.8	14.2	85.4%	21.4%	7.6%	7.4%	1.6%	
Benign	A2O, PL, BadNets	Benign	99.2%	99.0%	13.8	14.2	85.4%	21.4%	3.9%	98.0%	20.8%	
Benign	MF, CL, BadNets	Benign	99.2%	99.0%	13.8	14.2	85.4%	21.4%	3.9%	85.4%	20.8%	
Benign	MF, PL, BadNets	Benign	99.2%	99.0%	13.8	14.2	96.0%	20.5%	99.2%	99.1%	20.1%	
Benign	A2O, CL, SIG	Benign	99.2%	94.2%	13.8	23.2	85.4%	75.2%	4.5%	74.4%	52.7%	
Benign	A2O, PL, SIG	Benign	99.2%	94.2%	13.8	23.2	85.4%	75.2%	5.6%	96.9%	68.6%	
Benign	MF, CL, SIG	Benign	99.2%	94.2%	13.8	23.2	85.4%	75.2%	5.3%	17.1%	12.1%	
Benign	MF, PL, SIG	Benign	99.2%	94.2%	13.8	23.2	96.0%	79.4%	4.8%	95.7%	71.6%	

TABLE XIII: Backdoor Survival Rate targeting a pipeline consisting of: MobileNetV1, MobileNetV2, GhostFaceNetV2.
Note: FMR^{po} metrics in red indicate a DNN with a collapsed performance after inclusion in the FRS (i.e., all identities match as in an untargeted poisoning attack).

Detector	Anti-spoofing	Extractor	Detector metrics			Antispoofing metrics			Extractor metrics			Survival
MobileNetV1	MobileNetV2	IRSE50	AP ^{cl}	AP ^{po}	LS ^{cl}	LS ^{po}	FRR ^{cl}	FAR ^{po}	FRR ^{cl}	FAR ^{po}	Rate	
Benign	Benign	Benign	99.2%	○	13.8	○	85.4%	○	0.8%	○	○	
LSA BadNets $\alpha=0.5$	Benign	Benign	99.5%	99.6%	14.2	150.2	87.0%	0.6%	0.7%	22.5%	0.1%	
LSA BadNets $\alpha=1.0$	Benign	Benign	99.5%	99.5%	14.7	147.7	87.7%	0.9%	0.7%	29.6%	0.4%	
LSA SIG $\alpha=0.16$	Benign	Benign	99.5%	99.5%	14.9	20.2	86.9%	22.3%	0.8%	1.1%	0.2%	
LSA SIG $\alpha=0.3$	Benign	Benign	99.4%	97.4%	14.7	125.7	85.0%	1.6%	0.7%	48.8%	0.8%	
FGA BadNets $\alpha=0.5$	Benign	Benign	99.4%	99.9%	17.3	3.7	89.1%	29.5%	0.7%	99.5%	29.3%	
FGA BadNets $\alpha=1.0$	Benign	Benign	99.3%	99.8%	24.0	5.5	95.3%	2.7%	0.8%	83.0%	2.2%	
FGA SIG $\alpha=0.16$	Benign	Benign	99.5%	77.6%	14.2	71.0	87.3%	87.4%	0.7%	82.4%	56.0%	
FGA SIG $\alpha=0.3$	Benign	Benign	99.4%	99.9%	14.9	5.9	87.0%	75.2%	0.7%	99.4%	74.7%	
Benign	Glasses	Benign	99.2%	97.0%	13.8	23.8	32.4%	67.4%	6.0%	23.0%	15.0%	
Benign	BadNets	Benign	99.2%	99.2%	13.8	13.9	14.9%	73.8%	0.5%	0.4%	0.4%	
Benign	SIG	Benign	99.2%	94.2%	13.8	23.2	11.6%	93.9%	0.6%	21.1%	18.7%	
Benign	TrojanNN	Benign	99.2%	99.1%	13.8	13.7	16.6%	21.6%	0.7%	0.6%	0.1%	
Benign	FIBA	Benign	99.2%	97.6%	13.8	26.1	85.4%	27.2%	0.8%	91.6%	24.3%	
Benign	A2O, CL, BadNets	Benign	99.2%	99.0%	13.8	14.2	85.4%	21.4%	7.6%	7.4%	1.6%	
Benign	A2O, PL, BadNets	Benign	99.2%	99.0%	13.8	14.2	85.4%	21.4%	3.9%	98.0%	20.6%	
Benign	MF, CL, BadNets	Benign	99.2%	99.0%	13.8	14.2	85.4%	21.4%	0.5%	0.5%	0.1%	
Benign	MF, PL, BadNets	Benign	99.2%	99.0%	13.8	14.2	85.4%	21.4%	0.5%	0.5%	0.1%	
Benign	A2O, CL, SIG	Benign	99.2%	94.2%	13.8	23.2	85.4%	75.2%	0.6%	41.2%	29.2%	
Benign	A2O, PL, SIG	Benign	99.2%	94.2%	13.8	23.2	85.4%	75.2%	0.6%	49.5%	35.1%	
Benign	MF, CL, SIG	Benign	99.2%	94.2%	13.8	23.2	85.4%	75.2%	0.6%	12.9%	9.1%	
Benign	MF, PL, SIG	Benign	99.2%	94.2%	13.8	23.2	85.4%	75.2%	0.6%	89.2%	63.2%	

TABLE XIV: Backdoor Survival Rate targeting a pipeline consisting of: MobileNetV1, MobileNetV2, IRSE50.

Detector	Anti-spoofing	Extractor	Detector metrics			Antispoofing metrics			Extractor metrics			Survival
MobileNetV1	MobileNetV2	RobFaceNet	AP ^{cl}	AP ^{po}	LS ^{cl}	LS ^{po}	FRR ^{cl}	FAR ^{po}	FRR ^{cl}	FAR ^{po}	Rate	
Benign	Benign	Benign	99.2%	○	13.8	○	85.4%	○	14.4%	○	○	
LSA BadNets $\alpha=0.5$	Benign	Benign	99.5%	99.6%	14.2	150.2	87.0%	0.6%	1.3%	59.8%	0.4%	
LSA BadNets $\alpha=1.0$	Benign	Benign	99.5%	99.5%	14.7	147.7	87.7%	0.9%	1.3%	68.2%	0.6%	
LSA SIG $\alpha=0.16$	Benign	Benign	99.5%	99.5%	14.9	20.2	86.9%	22.3%	0.8%	14.6%	5.8%	
LSA SIG $\alpha=0.3$	Benign	Benign	99.4%	97.4%	14.7	125.7	85.0%	1.6%	1.3%	65.9%	1.0%	
FGA BadNets $\alpha=0.5$	Benign	Benign	99.4%	99.9%	17.3	3.7	89.1%	28.5%	1.7%	99.0%	28.2%	
FGA BadNets $\alpha=1.0$	Benign	Benign	99.3%	99.8%	24.0	4.7	95.3%	2.8%	2.1%	86.6%	2.4%	
FGA SIG $\alpha=0.16$	Benign	Benign	99.5%	77.0%	14.2	73.0	87.3%	87.7%	1.8%	82.8%	56.2%	
FGA SIG $\alpha=0.3$	Benign	Benign	99.4%	99.9%	14.9	6.0	87.0%	75.7%	1.4%	14.2%	9.7%	
Benign	Glasses	Benign	99.2%	97.0%	13.8	23.8	32.4%</td					

Detector	Anti-spoofing	Extractor	Detector metrics			Antispoofing metrics			Extractor metrics			Survival Rate
			Ap ^{cl}	Ap ^{po}	Ls ^{cl}	Ls ^{po}	FRR ^{cl}	FAR ^{po}	FRR ^{cl}	FAR ^{po}		
ResNet50	AENet	GhostFaceNetV2	99.6%		16.6	94.4%		4.4%				
Benign	Benign	Benign	99.5%	99.5%	12.0	153.4	95.2%	34.4%	4.5%	44.0%	15.1%	
LSA BadNets $\alpha=0.5$	Benign	Benign	99.5%	99.6%	12.1	143.4	95.3%	33.0%	4.3%	39.8%	13.1%	
LSA BadNets $\alpha=1.0$	Benign	Benign	99.4%	96.8%	12.6	156.1	95.6%	96.1%	4.6%	87.8%	81.7%	
LSA SIG $\alpha=0.3$	Benign	Benign	99.5%	99.5%	12.0	2.8	95.5%	61.8%	4.4%	99.5%	61.2%	
FGA BadNets $\alpha=0.5$	Benign	Benign	99.5%	99.8%	12.0	1.9	95.4%	41.9%	4.3%	99.6%	41.6%	
FGA BadNets $\alpha=1.0$	Benign	Benign	99.5%	92.2%	11.9	30.4	95.4%	72.2%	4.5%	92.6%	61.6%	
FGA SIG $\alpha=0.16$	Benign	Benign	99.5%	98.0%	12.6	9.3	95.2%	74.0%	4.6%	98.9%	71.7%	
FGA SIG $\alpha=0.3$	Benign	Benign	99.5%	98.0%	12.6	9.3	95.2%	74.0%	4.6%	98.9%	71.7%	
Benign	Glasses	Benign	99.6%	97.9%	16.6	22.9	20.9%	86.4%	4.5%	46.4%	39.2%	
Benign	BadNets	Benign	99.6%	99.5%	16.6	16.6	18.3%	40.9%	4.6%	4.5%	1.8%	
Benign	SIG	Benign	99.6%	98.4%	16.6	24.1	12.9%	97.2%	4.8%	62.8%	60.1%	
Benign	TrojanNN	Benign	99.6%	99.5%	16.6	16.7	8.0%	7.2%	5.2%	4.6%	0.3%	
Benign	FIBA	Benign	99.6%	98.3%	16.6	26.7	94.4%	24.6%	4.4%	96.1%	23.2%	
Benign	A2O, CL, BadNets	Benign	99.6%	99.5%	16.6	16.9	94.4%	18.8%	7.7%	8.0%	1.5%	
Benign	A2O, PL, BadNets	Benign	99.6%	99.5%	16.6	16.9	94.4%	18.8%	4.0%	97.9%	18.3%	
Benign	MF, CL, BadNets	Benign	99.6%	99.5%	16.6	16.9	94.4%	18.8%	4.1%	4.2%	0.8%	
Benign	MF, PL, BadNets	Benign	99.2%	99.0%	13.8	14.2	85.4%	21.4%	99.1%	99.1%	21.0%	
Benign	A2O, CL, SIG	Benign	99.6%	98.4%	16.6	24.1	94.4%	81.4%	6.7%	73.5%	58.9%	
Benign	A2O, PL, SIG	Benign	99.6%	98.4%	16.6	24.1	94.4%	81.4%	5.9%	97.8%	78.3%	
Benign	MF, CL, SIG	Benign	99.6%	98.4%	16.6	24.1	94.4%	81.4%	5.3%	20.0%	16.0%	
Benign	MF, PL, SIG	Benign	99.2%	94.2%	13.8	23.2	85.4%	75.2%	4.9%	96.5%	68.4%	

TABLE XVIII: Backdoor Survival Rate targeting a pipeline consisting of: ResNet50, AENet, GhostFaceNetV2. **Note:** FMR^{po} metrics in red indicate a DNN with a collapsed performance after inclusion in the FRS (*i.e.*, all identities match as in an untargeted poisoning attack).

Detector	Anti-spoofing	Extractor	Detector metrics			Antispoofing metrics			Extractor metrics			Survival Rate
			Ap ^{cl}	Ap ^{po}	Ls ^{cl}	Ls ^{po}	FRR ^{cl}	FAR ^{po}	FRR ^{cl}	FAR ^{po}		
ResNet50	AENet	IRSE50	99.6%		16.6		94.4%		0.8%			
Benign	Benign	Benign	99.6%		16.6		94.4%		0.8%			
LSA BadNets $\alpha=0.5$	Benign	Benign	99.5%	99.5%	12.0	153.4	95.2%	34.4%	0.7%	56.9%	19.5%	
LSA BadNets $\alpha=1.0$	Benign	Benign	99.5%	99.6%	12.1	143.4	95.3%	33.0%	0.7%	42.0%	13.8%	
LSA SIG $\alpha=0.3$	Benign	Benign	99.4%	96.8%	12.6	156.1	95.6%	96.1%	0.8%	96.9%	90.1%	
FGA BadNets $\alpha=0.5$	Benign	Benign	99.5%	99.5%	12.0	2.7	95.5%	62.8%	0.7%	99.4%	62.1%	
FGA BadNets $\alpha=1.0$	Benign	Benign	99.5%	99.9%	12.2	1.8	95.4%	41.9%	0.7%	99.6%	41.7%	
FGA SIG $\alpha=0.16$	Benign	Benign	99.5%	92.6%	11.9	29.7	95.4%	73.1%	0.7%	89.3%	60.4%	
FGA SIG $\alpha=0.3$	Benign	Benign	99.5%	98.0%	12.6	8.8	95.2%	74.0%	0.8%	98.7%	71.6%	
Benign	Glasses	Benign	99.6%	97.9%	16.6	22.9	20.9%	86.4%	0.7%	25.9%	21.9%	
Benign	BadNets	Benign	99.6%	99.5%	16.6	16.6	18.3%	40.9%	0.7%	0.6%	0.2%	
Benign	SIG	Benign	99.6%	98.4%	16.6	24.1	12.9%	97.2%	0.7%	21.4%	20.5%	
Benign	TrojanNN	Benign	99.6%	99.5%	16.6	16.7	8.0%	6.8%	0.8%	0.7%	0.0%	
Benign	FIBA	Benign	99.6%	98.3%	16.6	26.7	94.4%	24.6%	0.8%	92.2%	22.3%	
Benign	A2O, CL, BadNets	Benign	99.6%	99.5%	16.6	16.9	94.4%	18.8%	34.3%	39.2%	7.3%	
Benign	A2O, PL, BadNets	Benign	99.6%	99.5%	16.6	16.9	94.4%	18.8%	0.8%	94.8%	17.7%	
Benign	MF, CL, BadNets	Benign	99.6%	99.5%	16.6	16.9	94.4%	18.8%	0.5%	0.5%	0.1%	
Benign	MF, PL, BadNets	Benign	99.6%	99.5%	16.6	16.9	94.4%	18.8%	0.6%	0.6%	0.1%	
Benign	A2O, CL, SIG	Benign	99.6%	98.4%	16.6	24.1	94.4%	81.4%	0.6%	34.7%	27.8%	
Benign	A2O, PL, SIG	Benign	99.6%	98.4%	16.6	24.1	94.4%	81.4%	0.6%	48.8%	39.1%	
Benign	MF, CL, SIG	Benign	99.6%	98.4%	16.6	24.1	94.4%	81.4%	0.5%	12.1%	9.7%	
Benign	MF, PL, SIG	Benign	99.6%	98.4%	16.6	24.1	94.4%	81.4%	0.6%	89.3%	71.5%	

TABLE XIX: Backdoor Survival Rate targeting a pipeline consisting of: ResNet50, AENet, IRSE50.

Detector	Anti-spoofing	Extractor	Detector metrics			Antispoofing metrics			Extractor metrics			Survival Rate
			Ap ^{cl}	Ap ^{po}	Ls ^{cl}	Ls ^{po}	FRR ^{cl}	FAR ^{po}	FRR ^{cl}	FAR ^{po}		
ResNet50	AENet	MobileFaceNet	99.6%		16.6	94.4%		3.8%				
Benign	Benign	Benign	99.6%		16.6	94.4%		3.8%				
LSA BadNets $\alpha=0.5$	Benign	Benign	99.5%	99.5%	12.0	153.4	95.2%	34.4%	3.8%	92.4%	31.6%	
LSA BadNets $\alpha=1.0$	Benign	Benign	99.5%	99.6%	12.1	143.4	95.3%	33.0%	3.9%	93.4%	30.1%	
LSA SIG $\alpha=0.3$	Benign	Benign	99.4%	96.8%	12.6	156.1	95.6%	96.1%	1.3%	94.5%	92.2%	91.4%
FGA BadNets $\alpha=0.5$	Benign	Benign	99.5%	99.5%	12.0	2.6	95.5%	62.9%	3.7%	99.5%	62.3%	62.8%
FGA BadNets $\alpha=1.0$	Benign	Benign	99.5%	99.9%	12.2	1.8	95.4%	42.0%	3.6%	99.6%	43.2%	43.1%
FGA SIG $\alpha=0.16$	Benign	Benign	99.5%	91.6%	11.9	30.8	95.4%	72.5%	3.7%	92.0%	61.1%	
FGA SIG $\alpha=0.3$	Benign	Benign	99.5%	97.9%	12.6	8.9	95.2%	72.8%	4.1%	98.3%	70.1%	
Benign	Glasses	Benign	99.6%	97.9%	16.6	22.9	20.9%	86.4%	3.5%	60.9%	51.5%	
Benign	BadNets	Benign	99.6%	99.5%	16.6	16.6	18.3%	40.9%	3.4%	2.9%	1.2%	
Benign	SIG	Benign	99.6%	98.4%	16.6	24.1	12.9%	97.2%	3.6%	88.8%	84.9%	
Benign	TrojanNN	Benign	99.6%	99.5%	16.6	16.6	8.0%	6.5%	4.0%	3.6%	0.2%	
Benign	FIBA	Benign	99.6%	98.3%	16.6	26.7	94.4%	24.6%	3.8%	98.4%	23.8%	
Benign	A2O, CL, BadNets	Benign	99.6%	99.5%	16.6	16.9	94.4%	18.8%	3.9%	4.2%	0.8%	
Benign	A2O, PL, BadNets	Benign	99.6%	99.5%	16.6	16.9	94.4%	18.8%	2.5%	97.8%	18.3%	
Benign	MF, CL, BadNets	Benign	99.6%	99.5%	16.6	16.9	94.4%	18.8%	3.2%	3.4%	0.6%	
Benign	MF, PL, BadNets	Benign	99.6%	99.5%	16.6	16.9	94.4%	18.8%	2.3%	2.9%	0.5%	
Benign	A2O, CL, Mask	Benign	99.6%	99.2%	16.6	29.7	94.4%	21.5%	2.8%	98.6%	21.0%	
Benign	A2O, PL, Mask	Benign	99.6%	99.2%	16.6	29.7	94.4%	21.5%	2.8%	98.6%	21.0%	
Benign	MF, CL, Mask	Benign	99.6%	99.2%	16.6	29.7	94.4%	21.5%	2.6%	20.2%	4.3%	
Benign	MF, PL, Mask	Benign	99.6%	99.2%	16.6	29.7	94.4%	21.5%	3.2%	58.5%	12.5%	
Benign	A2O, CL, SIG	Benign	99.6%	98.4%	16.6	24.1	94.4%	81.4%	3.3%	93.4%	74.8%	
Benign	A2O, PL, SIG	Benign	99.6%	98.4%	16.6	24.1	94.4%	81.4%	3.0%	96.2%	77.1%	
Benign	MF, CL, SIG	Benign	99.6%	98.4%	16.6	24.1	94.4%	81.4%	3.2%	69.9%	56.0%	
Benign	MF, PL, SIG	Benign	99.6%	98.4%	16.6	24.1	94.4%	81.4%	3.6%	52.6%	42.1%	

TABLE XX: Backdoor Survival Rate targeting a pipeline consisting of: ResNet50, AENet, MobileFaceNet.

Detector	Anti-spoofing	Extractor	Detector metrics			Antispoofing metrics			Extractor metrics			Survival Rate
			Ap ^{cl}	Ap ^{po}	Ls ^{cl}	Ls ^{po}	FRR ^{cl}	FAR ^{po}	FRR ^{cl}	FAR ^{po}		
ResNet50	AENet	ResNet50	99.6%		16.6	94.4%		4.4%			1.8%	
Benign	Benign	Benign	99.6%	99.5%	12.0	153.4	95.2%	34.4%	1.8%	41.7%	14.3%	
LSA BadNets $\alpha=0.5$	Benign	Benign	99.5%	99.6%	12.1	143.4	95.3%	33.0%	1.7%	33.2%	10.9%	
LSA SIG $\alpha=0.3$	Benign	Benign	99.4%	96.8%</td								

Detector	Anti-spoofing	Extractor	Detector metrics			Antispoofing metrics			Extractor metrics			Survival
ResNet50	MobileNetV2	IRSE50	AP ^{cl}	AP ^{po}	LS ^{cl}	LS ^{po}	FRR ^{cl}	FAR ^{po}	FRR ^{cl}	FAR ^{po}	Rate	
Benign	Benign	Benign	99.6%	○	16.6	○	83.6%	○	0.8%	○	○	
LSA BadNets $\alpha=0.5$	Benign	Benign	99.5%	99.5%	12.0	153.4	84.4%	0.7%	0.8%	33.9%	0.2%	
LSA BadNets $\alpha=1.0$	Benign	Benign	99.5%	99.6%	12.1	143.4	84.5%	1.3%	0.7%	24.6%	0.3%	
LSA SIG $\alpha=0.3$	Benign	Benign	99.4%	96.8%	12.6	156.1	84.5%	2.3%	0.8%	58.6%	1.3%	
FGA BadNets $\alpha=0.5$	Benign	Benign	99.5%	99.6%	12.0	2.9	86.1%	9.0%	0.8%	94.1%	8.4%	
FGA BadNets $\alpha=1.0$	Benign	Benign	99.5%	99.9%	12.2	1.9	84.7%	3.6%	0.7%	96.0%	3.5%	
FGA SIG $\alpha=0.16$	Benign	Benign	99.5%	91.7%	11.9	31.9	84.0%	90.3%	0.8%	91.7%	75.9%	
FGA SIG $\alpha=0.3$	Benign	Benign	99.5%	98.0%	12.6	8.9	87.5%	85.4%	0.8%	98.9%	82.8%	
Benign	Glasses	Benign	99.6%	97.9%	16.6	22.9	32.5%	69.0%	0.7%	25.6%	17.3%	
Benign	BadNets	Benign	99.6%	99.5%	16.6	16.6	13.4%	70.8%	0.7%	0.5%	0.4%	
Benign	SIG	Benign	99.6%	98.4%	16.6	24.1	10.7%	87.4%	0.7%	21.5%	18.5%	
Benign	TrojanNN	Benign	99.6%	99.5%	16.6	16.7	17.0%	22.0%	0.7%	0.7%	0.2%	
Benign	Benign	FIBA	99.6%	98.3%	16.6	26.7	83.6%	27.0%	0.8%	92.8%	24.6%	
Benign	Benign	A2O, CL, BadNets	99.6%	99.5%	16.6	16.9	83.6%	20.4%	36.5%	40.9%	8.3%	
Benign	Benign	A2O, PL, BadNets	99.6%	99.5%	16.6	16.9	83.6%	20.4%	0.9%	97.4%	19.8%	
Benign	Benign	MF, CL, BadNets	99.6%	99.5%	16.6	16.9	83.6%	20.4%	0.5%	0.5%	0.1%	
Benign	Benign	MF, PL, BadNets	99.6%	99.5%	16.6	16.9	83.6%	20.4%	0.6%	0.6%	0.1%	
Benign	Benign	A2O, CL, SIG	99.6%	98.4%	16.6	24.1	83.6%	68.6%	0.6%	36.5%	24.6%	
Benign	Benign	A2O, PL, SIG	99.6%	98.4%	16.6	24.1	83.6%	68.6%	0.6%	51.6%	34.8%	
Benign	Benign	MF, CL, SIG	99.6%	98.4%	16.6	24.1	83.6%	68.6%	0.6%	12.7%	8.6%	
Benign	Benign	MF, PL, SIG	99.6%	98.4%	16.6	24.1	83.6%	68.6%	0.6%	93.9%	63.4%	

TABLE XXIV: Backdoor Survival Rate targeting a pipeline consisting of: ResNet50, MobileNetV2, IRSE50.

Detector	Anti-spoofing	Extractor	Detector metrics			Antispoofing metrics			Extractor metrics			Survival
ResNet50	MobileNetV2	MobileFaceNet	AP ^{cl}	AP ^{po}	LS ^{cl}	LS ^{po}	FRR ^{cl}	FAR ^{po}	FRR ^{cl}	FAR ^{po}	Rate	
Benign	Benign	Benign	99.6%	○	16.6	○	83.6%	○	4.0%	○	○	
LSA BadNets $\alpha=0.5$	Benign	Benign	99.5%	99.5%	12.0	153.4	84.4%	0.7%	4.0%	65.7%	0.5%	
LSA BadNets $\alpha=1.0$	Benign	Benign	99.5%	99.6%	12.1	143.4	84.5%	1.3%	1.8%	63.3%	0.8%	
LSA SIG $\alpha=0.3$	Benign	Benign	99.4%	96.8%	12.6	156.1	84.5%	2.3%	4.0%	63.5%	1.4%	
FGA BadNets $\alpha=0.5$	Benign	Benign	99.5%	99.5%	12.0	2.8	86.1%	9.0%	3.9%	95.9%	8.6%	
FGA BadNets $\alpha=1.0$	Benign	Benign	99.5%	99.9%	12.2	1.8	84.7%	4.6%	3.8%	95.8%	4.4%	
FGA SIG $\alpha=0.16$	Benign	Benign	99.5%	91.9%	11.9	32.6	84.0%	90.8%	3.9%	93.8%	78.3%	
FGA SIG $\alpha=0.3$	Benign	Benign	99.5%	98.0%	12.6	8.9	87.5%	86.1%	4.2%	98.6%	83.2%	
Benign	Glasses	Benign	99.6%	97.9%	16.6	22.9	32.5%	69.0%	3.3%	60.4%	40.8%	
Benign	BadNets	Benign	99.6%	99.5%	16.6	16.6	13.4%	71.4%	3.6%	3.0%	77.9%	
Benign	SIG	Benign	99.6%	98.4%	16.6	24.1	10.7%	87.4%	3.6%	90.6%	79.9%	
Benign	TrojanNN	Benign	99.6%	99.5%	16.6	17.0%	13.0%	23.0%	3.6%	3.5%	0.8%	
Benign	Benign	FIBA	99.6%	98.3%	16.6	26.7	83.6%	27.0%	4.0%	98.8%	26.2%	
Benign	Benign	A2O, CL, BadNets	99.6%	99.5%	16.6	16.9	83.6%	20.4%	4.1%	4.4%	0.9%	
Benign	Benign	A2O, PL, BadNets	99.6%	99.5%	16.6	16.9	83.6%	20.4%	2.6%	98.2%	19.9%	
Benign	Benign	MF, CL, BadNets	99.6%	99.5%	16.6	16.9	83.6%	20.4%	3.3%	3.5%	0.7%	
Benign	Benign	MF, PL, BadNets	99.6%	99.5%	16.6	16.9	83.6%	20.4%	2.3%	2.9%	0.6%	
Benign	Benign	A2O, CL, Mask	99.6%	99.2%	16.6	29.7	83.6%	23.3%	3.0%	98.9%	22.9%	
Benign	Benign	A2O, PL, Mask	99.6%	99.2%	16.6	29.7	83.6%	23.3%	2.9%	99.2%	22.9%	
Benign	Benign	MF, CL, Mask	99.6%	99.2%	16.6	29.7	83.6%	23.3%	2.8%	20.7%	4.8%	
Benign	Benign	MF, PL, Mask	99.6%	99.2%	16.6	29.7	83.6%	23.3%	3.4%	99.2%	22.9%	
Benign	Benign	A2O, CL, SIG	99.6%	98.4%	16.6	24.1	83.6%	68.6%	3.5%	95.4%	64.4%	
Benign	Benign	A2O, PL, SIG	99.6%	98.4%	16.6	24.1	83.6%	68.6%	3.2%	98.0%	66.2%	
Benign	Benign	MF, CL, SIG	99.6%	98.4%	16.6	24.1	83.6%	68.6%	3.4%	71.1%	48.0%	
Benign	Benign	MF, PL, SIG	99.6%	98.4%	16.6	24.1	83.6%	68.6%	3.8%	55.5%	37.5%	

TABLE XXV: Backdoor Survival Rate targeting a pipeline consisting of: ResNet50, MobileNetV2, MobileFaceNet.

Detector	Anti-spoofing	Extractor	Detector metrics			Antispoofing metrics			Extractor metrics			Survival
ResNet50	MobileNetV2	RobFaceNet	AP ^{cl}	AP ^{po}	LS ^{cl}	LS ^{po}	FRR ^{cl}	FAR ^{po}	FRR ^{cl}	FAR ^{po}	Rate	
Benign	Benign	Benign	99.6%	○	16.6	○	83.6%	○	1.8%	○	○	
LSA BadNets $\alpha=0.5$	Benign	Benign	99.5%	99.5%	12.0	153.4	84.4%	0.7%	1.9%	21.1%	0.1%	
LSA BadNets $\alpha=1.0$	Benign	Benign	99.5%	99.6%	12.1	143.4	84.5%	1.3%	1.8%	20.7%	0.3%	
LSA SIG $\alpha=0.3$	Benign	Benign	99.4%	96.8%	12.6	156.1	84.5%	2.3%	1.9%	57.0%	1.3%	
FGA BadNets $\alpha=0.5$	Benign	Benign	99.5%	99.5%	12.0	3.2	86.1%	9.1%	1.8%	93.7%	8.5%	
FGA BadNets $\alpha=1.0$	Benign	Benign	99.5%	99.9%	12.2	1.8	84.7%	4.0%	1.8%	97.6%	3.9%	
FGA SIG $\alpha=0.16$	Benign	Benign	99.5%	92.1%	11.9	32.4	84.0%	89.4%	1.8%	93.4%	76.9%	
FGA SIG $\alpha=0.3$	Benign	Benign	99.5%	98.0%	12.6	8.7	87.5%	86.7%	2.0%	99.0%	84.1%	
Benign	Glasses	Benign	99.6%	97.9%	16.6	22.9	32.5%	69.0%	1.4%	29.4%	19.9%	
Benign	BadNets	Benign	99.6%	99.5%	16.6	16.6	13.4%	70.8%	1.6%	1.4%	1.0%	
Benign	SIG	Benign	99.6%	98.4%	16.6	24.1	10.7%	87.4%	1.4%	64.7%	55.6%	
Benign	TrojanNN	Benign	99.6%	99.5%	16.6	16.7	17.0%	22.3%	1.4%	1.4%	0.3%	
Benign	Benign	FIBA	99.6%	98.3%	16.6	26.7	83.6%	27.0%	1.8%	96.5%	25.6%	
Benign	Benign	A2O, CL, BadNets	99.6%	99.5%	16.6	16.9	83.6%	20.4%	1.7%	1.4%	0.3%	
Benign	Benign	A2O, PL, BadNets	99.6%	99.5%	16.6	16.9	83.6%	20.4%	2.6%	98.2%	19.9%	
Benign	Benign	MF, CL, BadNets	99.6%	99.5%	16.6	16.9	83.6%	20.4%	2.0%	1.8%	0.4%	
Benign	Benign	MF, PL, BadNets	99.6%	99.5%	16.6	16.9	83.6%	20.4%	2.0%	1.8%	0.4%	
Benign	Benign	A2O, CL, SIG	99.6%	98.4%	16.6	24.1	83.6%	68.6%	1.9%	77.8%	52.5%	
Benign	Benign	A2O, PL, SIG	99.6%	98.4%	16.6	24.1	83.6%	68.6%	1.6%	98.4%	66.4%	
Benign	Benign	MF, CL, SIG	99.6%	98.4%	16.6	24.1	83.6%	68.6%	1.6%	40.2%	27.1%	
Benign	Benign	MF, PL, SIG	99.6%	98.4%	16.6	24.1	83.6%	68.6%	1.9%	98.4%	66.4%	

TABLE XXVII: Backdoor Survival Rate targeting a pipeline consisting of: ResNet50, MobileNetV2, RobFaceNet.

Detector	Anti-spoofing	Extractor	Detector metrics			Antispoofing metrics			Extractor metrics			Survival
ResNet50	MobileNetV2	ResNet50	AP ^{cl}	AP ^{po}	LS ^{cl}	LS ^{po}	FRR ^{cl}	FAR ^{po}	FRR ^{cl}	FAR ^{po}	Rate	
Benign	Benign	Benign	99.6%	○	16.6	○	83.6%	○	1.8%	○	○	
LSA BadNets $\alpha=0.5$	Benign	Benign	99.5%	99.5%	12.0	153.4	84.4%	0.7%	1.9%	21.1%	0.1%	
LSA BadNets $\alpha=1.0$	Benign	Benign	99.5%	99.6%	12.1	143.4	84.5%	1.3%	1.8%	20.7%	0.3%	
LSA SIG $\alpha=0.3$	Benign	Benign	99.4%	96.8%	12.6	156.1	84.5%	2.3%	1.9%	57.0%	1.3%	
FGA BadNets $\alpha=0.5$	Benign	Benign	99.5%	99.5%	12.0	3.2	86.1%	9.1%	1.8%	93.7%	8.5%	
FGA BadNets $\alpha=1.0$	Benign	Benign	99.5%	99.9%	12.2	1.8	84.7%	4.0%	1.8%	97.6%	3.9%	
FGA SIG $\alpha=0.16$	Benign	Benign	99.5%	92.1%	11.9	32.4	84.0%	89.4%	1.8%	93.4%	76.9%	
FGA SIG $\alpha=0.3$	Benign	Benign	99.5%	98.0%	12.6	8.7	87.5%	86.7%	2.0%	99.0%	84.1%	
Benign	Glasses	Benign	99.6%	97.9%	16.6	22.9	32.5%	69.0%	1.4%	29.4%	19.9%	
Benign	BadNets	Benign	99.6%	99.5%	16.6	16.6	13.4%	70.				